

Rochester Institute of Technology

RIT Digital Institutional Repository

Theses

2005

A Process Capability Index for Three-Dimensional Data with Circular or Ellipsoidal Tolerances.

Veljko Fotak

Follow this and additional works at: <https://repository.rit.edu/theses>

Recommended Citation

Fotak, Veljko, "A Process Capability Index for Three-Dimensional Data with Circular or Ellipsoidal Tolerances." (2005). Thesis. Rochester Institute of Technology. Accessed from

This Thesis is brought to you for free and open access by the RIT Libraries. For more information, please contact repository@rit.edu.

**A Process Capability Index for Three-Dimensional Data with
Circular or Ellipsoidal Tolerances.**

Veljko Fotak

December, 2005

**A Thesis Submitted to the Faculty of the Center for Quality and
Applied Statistics in Partial Fulfillment of the Requirements for
the Degree of MASTER OF SCIENCE in Applied Statistics.**

Prof. Joseph G. Voelkel

(Thesis advisor)

Prof. Daniel R. Lawrence

Prof. Steven LaLonde

Prof. Illegible Signature

(Department Head)

THESIS RELEASE PERMISSION FORM

ROCHESTER INSTITUTE OF TECHNOLOGY COLLEGE OF ENGINEERING

Title of Thesis:

A Process Capability Index for Three-Dimensional Data with Circular
or Ellipsoidal Tolerances.

I, Veljko Fotak, hereby grant permission to the Wallace Memorial Library of R.I.T. to reproduce my thesis in whole or in part. Any reproduction should not be for commercial use or profit.

Signature Veljko Fotak

Date: December 1, 2005

Table of Contents

A Process Capability Index for Three-Dimensional Data with Circular or Ellipsoidal Tolerances.....	1
Thesis Release Permission Form.....	2
Table of Contents.....	3
Table of Figures.....	4
Abstract.....	5
Why a single-numerical measure.....	6
The proposed process capability index.....	8
Gauge R&R in three dimensions.....	11
Literature review.....	13
Other process capability indices.....	15
Calculating the summary measure of variability.....	21
A geometric interpretation of the procedure presented.....	24
Estimating c and calculating the multivariate process capability index.....	28
Estimating M	31
Extensions to p dimensions.....	32
Application: analysis of color metrics.....	33
Applications.....	39
Example 1.....	42
Example 2.....	51
Example 3.....	57
Appendix 1.....	64
The function Rub	66
The function $Invrub$	68
Appendix 2.....	69
The function Pci	71
Appendix 3. Data assumption checking, instrument I, long-term data, cyan.....	73
References.....	82

Table of Figures

Figure 1. Tolerance region and smallest .99 capture ellipse 9

Figure 2. Tolerance region and proposed .99 capture ellipse 10

Figure 3. Data and tolerance region with similar orientations..... 17

Figure 4. Data and tolerance region with different orientations. 18

Figure 5. Data and tolerance region with different orientations and fitted capture ellipsoid. 19

Figure 6. Tolerance, data and fitted ellipse..... 25

Figure 7. Transformation to “U-space”. 26

Figure 8. Transformation to “V-space”. 27

Figure 9. Process capability indices, Example 1..... 46

Figure 10. Data, tolerance and fitted ellipsoid, Example 1..... 48

Figure 11. Tolerance and natural .99 capture ellipsoids for each var. component,
 Example 1. 49

Figure 12. Tolerance and fitted .99 capture spheres for each var. component, Example 1.... 50

Figure 13. Process capability index, Example 2..... 53

Figure 14. Data and tolerance region, instrument A, Example 2..... 55

Figure 15. Tolerance region and fitted .99 capture spheres for each variance component,
 instrument A, Example 2. 56

Figure 16. Process capability indices, Example 3..... 61

Figure 17. Data and tolerance region, instrument A, Example 3..... 62

Figure 18. Tolerance, .99 natural capture ellipsoid and .99 capture fitted ellipsoid, instrument
 A, Example 3. 63

Figure 19. Output of the *Pci* algorithm..... 71

Figure 20. Lightness versus time, long-term, cyan, instrument I. 74

Figure 21. Chroma versus time, long-term, cyan, instrument I. 75

Figure 22. Hue versus time, long-term, cyan, instrument I. 76

Figure 23. Normal probability plot, long-term, cyan, instrument I, lightness. 78

Figure 24. Normal probability plot, long-term, cyan, instrument I, chroma. 79

Figure 25. Normal probability plot, long-term, cyan, instrument I, hue..... 80

Figure 26. Chi-square Q-Q plot, long term, cyan, instrument I..... 81

Abstract

We discuss the estimation of a process capability index for three-dimensional data. Initially, we focus on the case in which the engineering tolerance associated with the measurements is a sphere. Then, we extend the discussion to the more general case in which the engineering tolerance is ellipsoidal. In both cases, we develop summary measures for repeatability and reproducibility, to be used in the context of a process capability index.

In the spherical tolerance case we define summary measures, where each measure is based on the diameter of a sphere that leads to a pre-specified capture rate (we will use here 99%). As a process capability index, we propose ratios, where each ratio is the diameter of such a sphere divided by the diameter of the tolerance sphere.

In the ellipsoidal tolerance case, such summary measure will be based on the length of the major axes of the ellipsoid of identical shape and orientation to the tolerance ellipsoid providing a pre-specified capture rate (again, we will use here 99%). As a process capability index, we propose ratios, where each ratio is the major axis of such ellipsoid divided by the major axis of the tolerance ellipsoid.

We present two algorithms in the language R aimed at facilitating the estimation of our summary measure of variability. The first algorithm evaluates the probability that a linear combination of three (or fewer) independent chi-square variables will be less than or equal to a given constant. The second algorithm estimates the value a linear combination of chi-square variables is less than or equal to, given a pre-specified probability. In addition, we

offer an algorithm in the language R for computing the process capability index in the context of color metrics.

We present applications to color measurements and to R&R analysis of color metrics.

We show how the components of variance in these three-dimensional measurements can be easily compared to each other and to the tolerance region, using the single-dimensional summary measures of process capability.

Why a single-numerical measure

In the single-sample trivariate normal case, six numbers (three variances and three covariances) are needed to describe the variability. We suggest here the use of a single-numerical summary measure of variability, mainly to be used within the context of a process capability index, to replace those six numbers.

While the use of a single-dimensional measure of variability necessarily leads to a partial loss of information, there are various advantages of using such univariate measure:

- Such a summary measure allows for an easy and intuitive comparison of the observed variability in relation to the defined tolerance region. An appropriate ratio of the observed variability to the tolerance offers a meaningful estimate of the amount of tolerance “used” by each component of variance.

- Similarly, such a summary measure offers an easy and intuitive comparison of the relative magnitudes of the estimated components of variance (allowing for the identification and comparison of major sources of variation). This measure can then be used to prioritize corrective actions, if needed.
- A univariate summary measure allows for other kinds of comparisons of variance components, depending on the particular applications. In the colorimetric example that we provide, the univariate measure of variability offers intuitive means to compare instruments in terms of the observed variability.
- The proposed measure of variability is easier to comprehend than the six-number variance-covariance matrix.

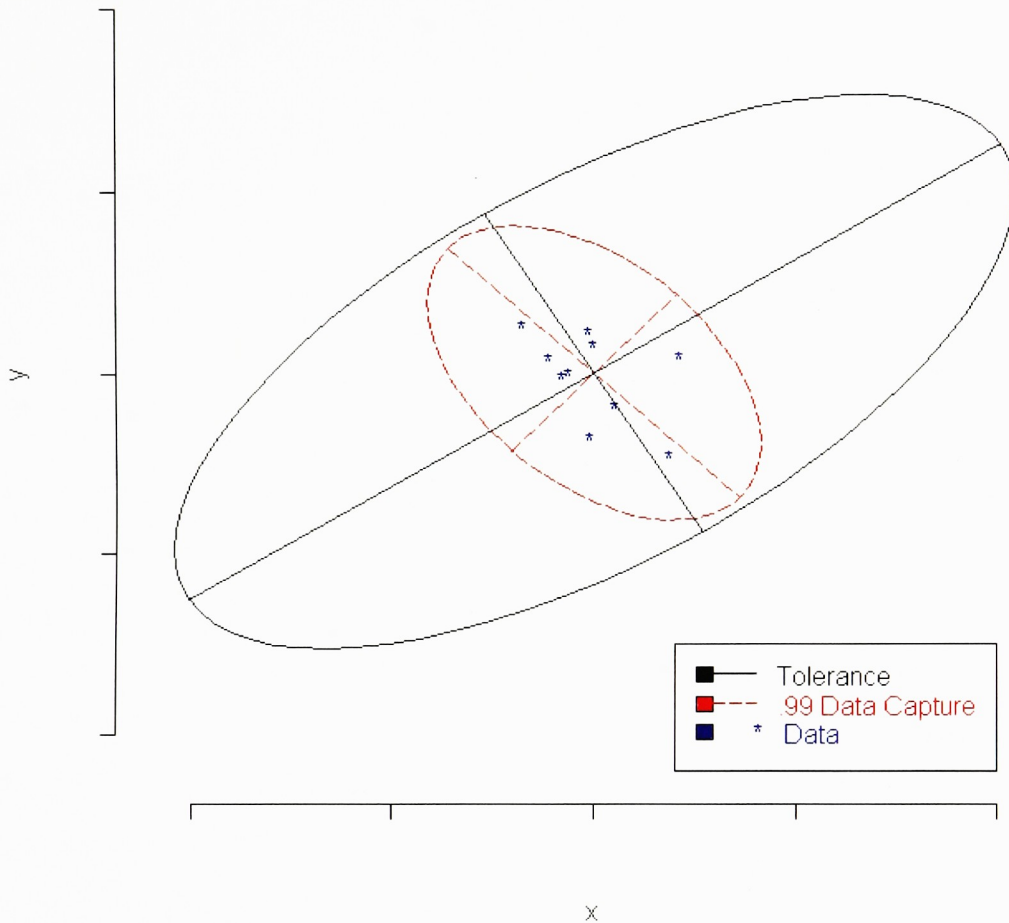
Depending on the application, other summary measures, or even direct analysis of the variance-covariance matrix, might be preferred in estimating process capability.

The proposed process capability index

In the case of spherical tolerances, we propose to fit a sphere that provides a pre-specified capture rate to the data. Our proposed process capability index can then be computed as the ratio between the diameter of this fitted spheroid and the diameter of the tolerance spheroid. As discussed in the *Other process capability indices* section, other metrics derived from such spheres have been proposed in the past (most notably, the volumes), but most methods agree in fitting a sphere providing a predetermined capture rate.

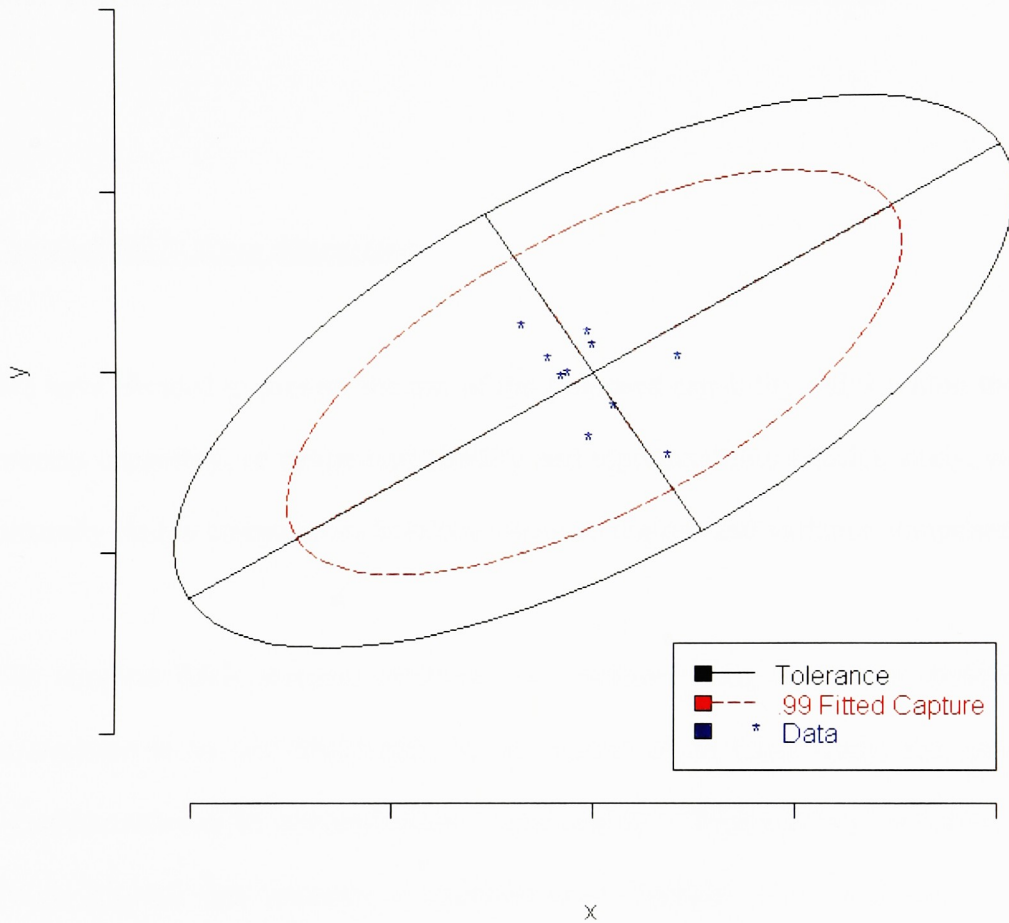
In the case of ellipsoidal tolerances, as discussed in more detail in the *Literature Review* section, it is common practice to base an estimation of process capability on some measure relative to the smallest ellipsoid that provides a particular capture rate - for example, by comparing the length of the major axis of said ellipsoid to the length of the major axis of the tolerance ellipsoid. A two-dimensional representation is available in Figure 1. The smallest ellipsoid providing a pre-determined capture rate is what would commonly be used to derive a process capability index.

Figure 1. Tolerance region and smallest .99 capture ellipse.



In contrast, we recommend using a different ellipsoid – that is, the ellipsoid with the same shape and orientation of the tolerance ellipsoid that provides a particular capture rate (we offer an example in two dimensions in Figure 2).

Figure 2. Tolerance region and proposed .99 capture ellipse.



We will refer to the smallest fitted ellipsoid (presented in Figure 1) as “data capture”, or “natural”, ellipsoid and to the fitted ellipsoid of same shape and orientation as the tolerance (as in Figure 2) as “fitted capture”, or “fitted” ellipsoid.

In the case of ellipsoidal tolerances, we propose the use of the major axis of the ellipsoid of the same shape and orientation as the tolerance ellipsoid as a summary measure of

variability. However, for the purposes of a process capability index, the choice of which axis to use leads to invariant results. That is, given that the shape of the compared ellipsoids is identical, the ratio of the major axes is identical to the ratio of the minor axes – or, in the more general case, to the ratio of any other corresponding pair of axes.

Gauge R&R in three dimensions

We have decided to present the use of the proposed capability index within the context of a process capability, or gauge repeatability and reproducibility (R&R), study, as such studies naturally lead to comparisons between tolerance regions and variance components.

The simplest R&R scenario involves one operator, using one gauge, making a series of measurements on one single part. In the context of an R&R study, the variation of such measurements can be summarized by “repeatability”. “Repeatability” is defined as the length of an interval that captures a predetermined fraction γ (we will use $\gamma = .99$) of such measurements. In the case with spherical tolerance, we estimate repeatability as the length of the diameter of the sphere that captures a predetermined fraction γ of the reported readings collected by one operator, using one gauge, on one single part.

In R&R studies, it may be possible to further subset repeatability into additive components labeled “short-term repeatability”, “medium-term repeatability” and “long term repeatability”. Our summary measures of repeatability can be subset accordingly.

If we are to consider a scenario in which one of the above factors (operator or gauge) changes, we fall under the realm of “reproducibility”. “Reproducibility” is defined as the length of an interval that captures a predetermined fraction γ (we will use $\gamma = .99$) of such measurements. For example, if we consider multiple operators, using one gauge, each making a series of measurements on one single part, we obtain a variation that is conventionally labeled as “operator reproducibility”. Alternatively, “reproducibility” can refer to the case in which we have one operator using multiple gauges, or instruments, to make a series of measurements on one single part; in this case, we speak of “inter-instrument reproducibility”.

In the three-dimensional case with a spherical tolerance, we estimate “operator reproducibility” as the length of the diameter of the sphere that captures a predetermined fraction γ of the reported readings collected by multiple operators, using one gauge, on one single part. “Inter-instrument reproducibility” will be similarly estimated as the length of the diameter of the sphere that captures γ of the reported readings collected by one operator, using multiple gauges, on one single part – and so on, for whatever component of “reproducibility” is of interest.

In the more general case of elliptical tolerances, we extend the definitions of both repeatability and reproducibility; that is, we estimate repeatability as the length of the major axis of the ellipsoid of equal shape and orientation to the tolerance ellipse that captures γ of the reported readings collected by one operator, using one gauge, on one single part. “Operator-reproducibility” can then be similarly defined as the length of the major axis of the

ellipsoid - of equal shape and orientation to the tolerance ellipse - that captures γ of the reported readings collected by multiple operators, using one gauge, on one single part. “Inter-instrument reproducibility” can then be similarly estimated as the length of the major axis of the ellipsoid - of equal shape and orientation to the tolerance ellipse - that captures γ of the reported readings collected by one operator, using multiple gauges, on one single part – and so on, for whatever component of “reproducibility” is of interest.

Those components of variance (repeatability and reproducibility) including possible interactions (such as, an “operator - short term” interaction) can be estimated using the standard MANOVA method of moments. We offer some examples in the following sections.

Literature review

This thesis extends the work of Voelkel (2003), who examined the two-dimensional R&R analysis in the case when the specified tolerance was circular.

General theory behind gauge R&R studies can be found in AIAG (1992), Wheeler and Lyday (1989) and Burdick, Borror and Montgomery (2005).

The application presented here is related to color metrics. Völz (1995) discusses multivariate analysis of color metrics.

The process described falls under the wider category of “coverage problems”, discussed by Guenther and Terragno (1964).

The estimation of our summary measure of variability requires the estimation of the probability that a non-negative linear combination of independent chi-square variables will be smaller than or equal to a given constant. The same distribution of quadratic forms, with relative application, has been discussed in various different contexts. Johnson, Kotz and Balakrishnan (1998) offer an extensive discussion of the existing literature on the topic.

The distribution of a linear combination of χ^2 random variables, in particular, has been discussed and tabulated by Grad and Solomon (1955), by Solomon (1960) and by Marsiglia (1960) in the bi- and tri-variate cases. Johnson and Kotz (1968) presented tables for 4 and 5 dimensions and Solomon and Stephens (1977) offered tables based on linear combination of 6, 8 and 10 variables.

The ideas proposed by Solomon were developed into a series of algorithms; in particular, Sheil and O’Muircheartaigh (1977) offer an algorithm (AS 106) to calculate the probability that a linear combination of k non-central independent χ^2 random variables will be less than or equal to a constant c . Davies (1980) offers an algorithm (AS 155) with the same functionality, but employs inversion of the characteristic function to obtain the solution, based on a previously published paper by the same author (Davis (1973)). Farebrother (1984) offers an improved version (AS 204) to the algorithm AS 106, leading to generally faster computing times. The algorithms AS 155 and AS 204 are both based on a method outlined by Ruben (1962). Johnson, Kotz and Balakrishnan (1998) discuss other approaches that have

been employed to estimate the distribution function of a linear combination of chi-square variables.

Other process capability indices.

Voelkel (2003) discusses some summary measures of variability that have been considered in the past. The discussion is specific to the case in two dimensions, but the concepts apply similarly to our case.

In particular, the area of an ellipse of equal shape and orientation to the tolerance ellipse has been proposed by Hulting (1992). We believe this summary measure of variability to have one major difficulty in interpretation. While this area-based measure is mathematically equivalent to the circle-diameter measure, in most applications the users are more often thinking in terms of original units of measure, rather than in terms of the squared (or cubed) units associated with tolerance surfaces and volumes. The sphere-diameter measure that we propose is expressed in the original units of the measurements, thus offering more intuitive interpretations.

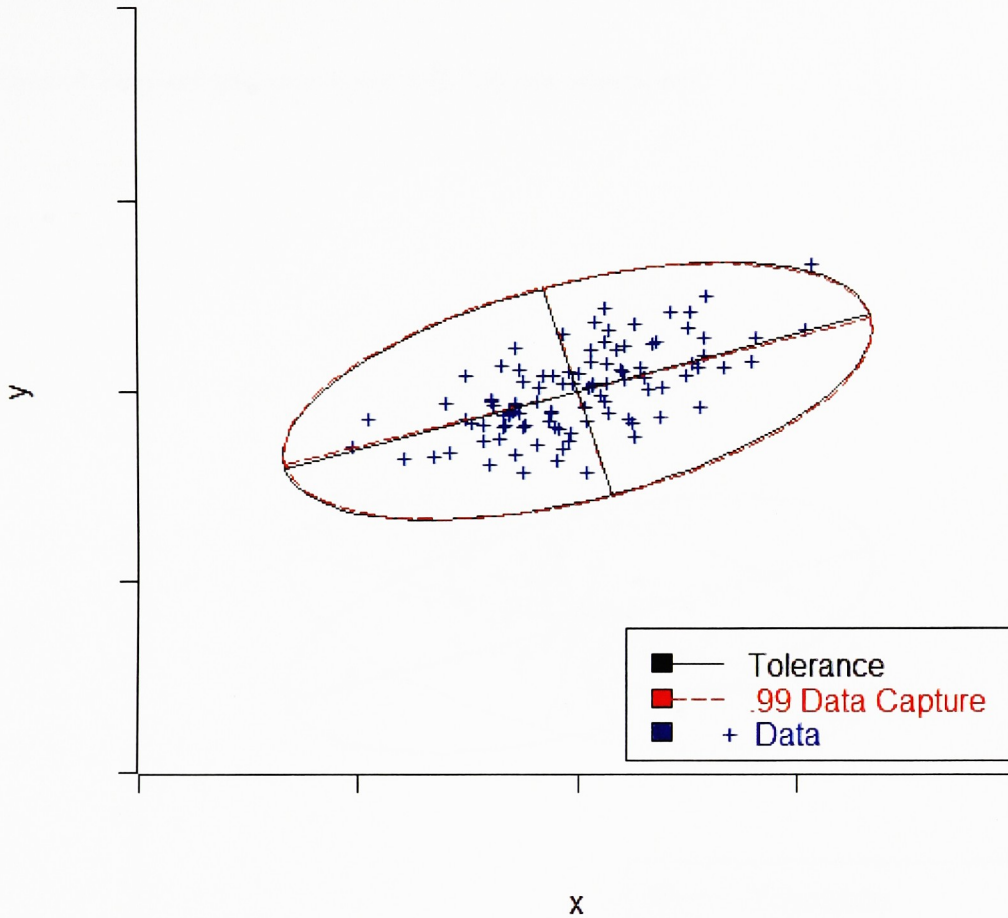
The length of the major axis of the natural ellipse providing a specific capture rate (Hulting (1992) and Demeter (1989)) has some appeal as it is a very intuitive summary measure of variability. We discuss here why we consider it an ineffective summary measure to be used within the context of a process capability index.

When the defined tolerance is spherical, there is no difference between the length of the diameter of the “natural” sphere providing a certain capture rate and the length of the diameter of the fitted sphere providing the same capture rate, as the two will be necessarily equivalent. On the other hand, with an ellipsoidal tolerance, a comparison of the length of the major axis of the ellipsoid offering a specific capture rate could, potentially, offer misleading results.

We will illustrate the possibility of misleading results in two dimensions. Consider a two-dimensional dataset with its smallest, or natural, .99 data capture ellipsoid. Assume that the size and shape of said ellipsoid are very similar to the size and shape of the tolerance ellipsoid. If, for example, the direction of maximum variability of the data was perfectly aligned with the direction of maximum variability of the tolerance region, as in Figure 3, a ratio of the major axis of the data and tolerance ellipses close to 1 would appear to suggest that the observed variability is about the same size of the tolerance region, leading to an acceptable product, or process. The dataset depicted includes 100 data points. As expected, given a capture rate of .99, we can observe that one point falls outside of our .99 data capture ellipsoid and outside the tolerance region.

Please note, a ratio larger than 1 would indicate that the proportion of observations falling within the tolerance is smaller than the predetermined capture rate (.99). A ratio smaller than 1 would indicate that the proportion of observations falling within the tolerance is larger than the predetermined capture rate (.99). A process capability index smaller than 1 is thus desirable.

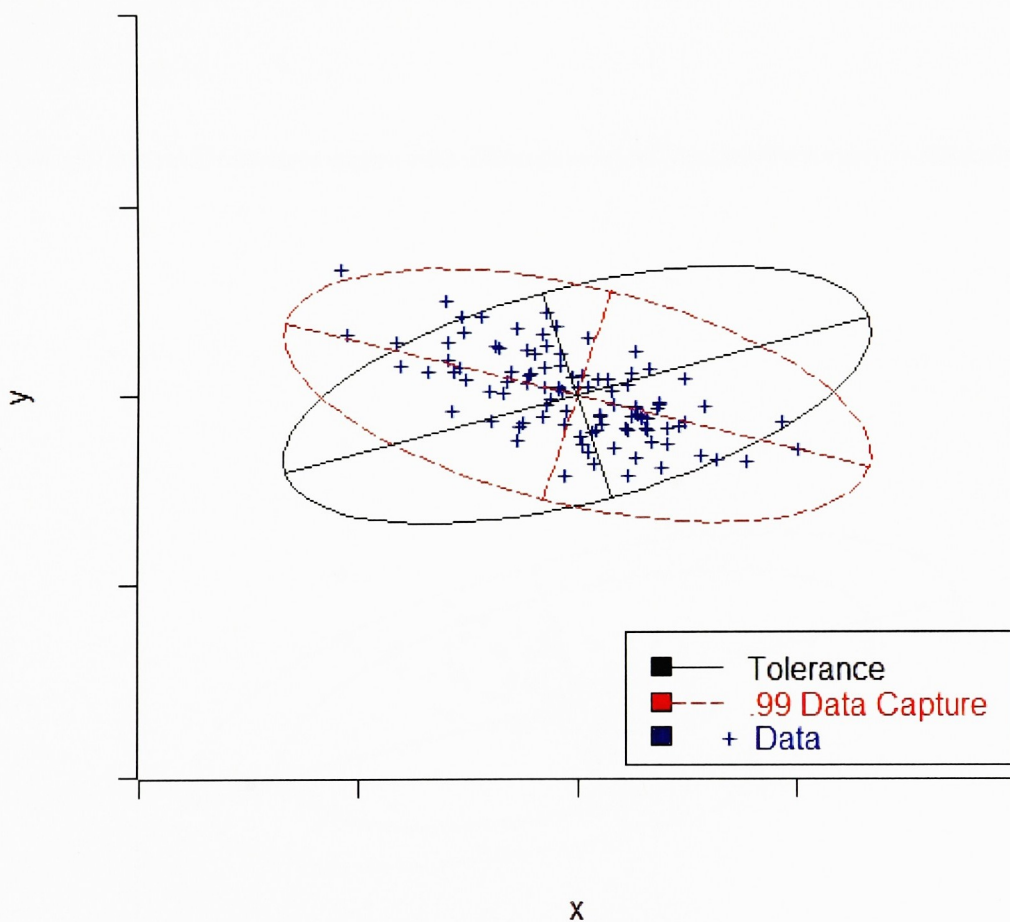
Figure 3. Data and tolerance region with similar orientations.



If, on the other side, the direction of maximum variability of the data was not aligned with the tolerance region, as in Figure 4, any ratio based on a comparison of lengths or surfaces of the two depicted ellipses would still be approximately 1, but the number of observations falling outside of the tolerance region would be considerably higher. In our example, only one observation falls outside of the .99 capture ellipsoid, but 7 observations fall outside the tolerance region. Clearly, the process capability indices for the cases in Figure 3 and Figure 4

should differ – since, in Figure 4, the tolerance region fails to capture .99 of the data, we would want the associated process capability index to be larger than 1.

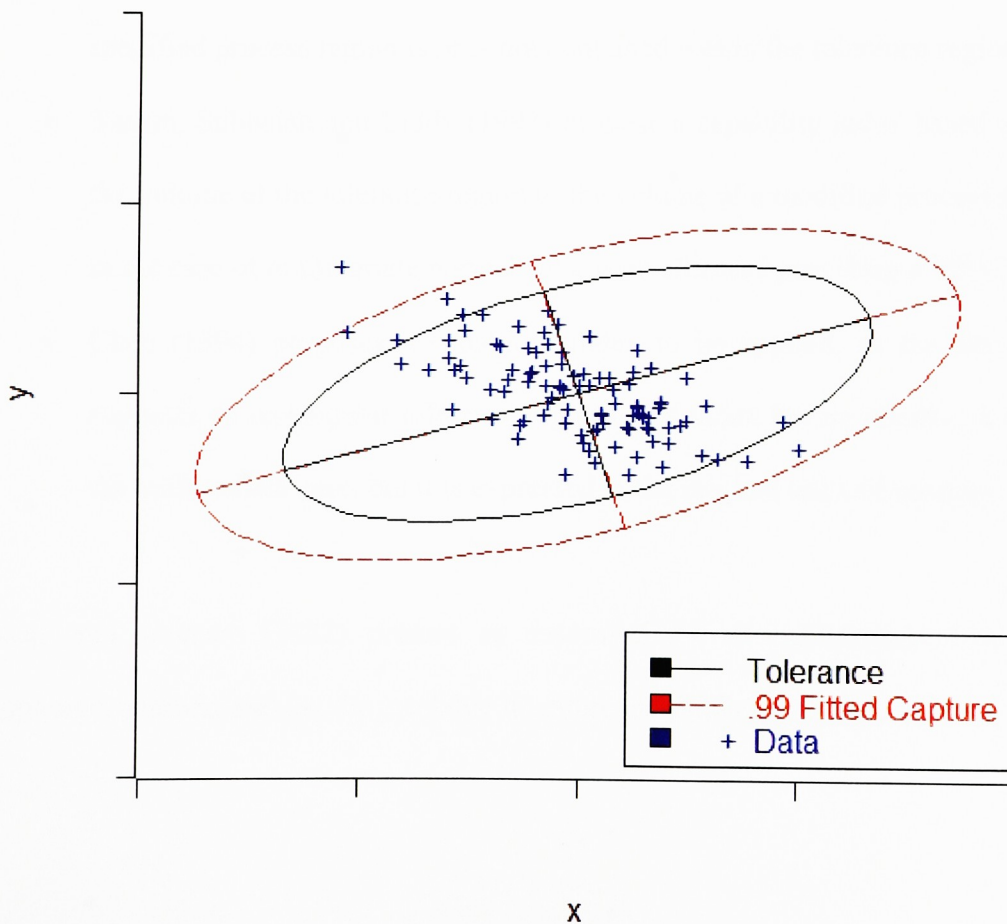
Figure 4. Data and tolerance region with different orientations.



The summary measure of variability we discuss also uses the major-axis length, but it does account for the differences in orientation between the data and tolerance region, thus being preferred in most applications. Given the same scenario as the one presented in Figure 4, when computing a process capability index, we would fit the capture ellipse presented in

Figure 5. The ratio of the length of the major axis of said ellipse to the length of the major axis of the tolerance ellipse is approximately 1.3 – indicating, correctly, that the process variability is indeed larger than the tolerance region. In this example, the predetermined capture rate is .99, but the tolerance region only captures 93% of the data; with out methodology, the associated process capability index is correctly estimated as being larger than one.

Figure 5. Data and tolerance region with different orientations and fitted capture ellipsoid.



Wang et al. (2000) discuss three other multivariate process capability indices (we cite the relevant indices in three-dimensional applications, although all three have been presented in a more general multivariate setting):

- Shahriari, Hubele and Lawrence (1995) propose a capability index based on three components: a ratio of volumes (the numerator being the volume defined by the engineering tolerance region and the denominator being the volume of a modified process region – the smallest region similar in shape to the engineering tolerance region, circumscribed around a probability contour), a measure of the distance of the centers of the tolerance and data regions and an index variable indicating whether the modified process region is or is not contained within the tolerance regions.
- Taaam, Subbaiah and Liddy (1993) propose a capability index based on the ratio of the volume of the tolerance region to the volume of a modified process region (which, in the case of multivariate normal data, is an ellipsoid providing a 99% capture rate).
- Chen (1994) proposes a capability index to be applied, as the title of his paper suggests, to rectangular tolerance regions. His index has no intuitive interpretation in the multivariate case, but it is expressed in the original units of measure of the data.

Kotz and Johnson (2002) present an extensive list of publications regarding process capability indices, and list the available literature on multivariate indices.

Calculating the summary measure of variability

Consider the simplest case of one operator, using one gauge, making a series of measurements on one single part, in which we want to estimate repeatability.

We assume that the variation in these measurements can be modeled by a multivariate (trivariate) normal distribution, which, without loss of generality, we assume is centered at zero:

$$\mathbf{X} \sim N_3(\mathbf{0}, \Sigma_x).$$

We also assume that the given tolerance region is a tri-dimensional ellipsoid (or, in a special case, a sphere) centered at zero. An ellipsoid can be mathematically described by: $\{\mathbf{x} : \mathbf{x}'\mathbf{M}\mathbf{x} = c^2\}$, where \mathbf{M} is a non-negative definite symmetric matrix defining the shape of the ellipsoid and c is a scale factor. For the tolerance ellipsoid, we set $c=1$, which reduces the equation of the tolerance ellipsoid to $\{\mathbf{x} : \mathbf{x}'\mathbf{M}\mathbf{x} = 1\}$. The tolerance region can then be described as the series of points $\{\mathbf{x} : \mathbf{x}'\mathbf{M}\mathbf{x} \leq 1\}$.

Please note that, for the present purposes, an ellipsoidal and a spherical tolerance region are treated in the same manner.

In order to compute our summary measure of variability, we aim at fitting an ellipsoid with the same shape and orientation as those of the tolerance ellipsoid, so that a certain proportion (the “capture rate”) of the observed data falls within the ellipse itself; that is, we want to find c such that:

$$P(\mathbf{X}'\mathbf{M}\mathbf{X} \leq c^2) = \gamma, \text{ where } \gamma \text{ is the desired capture rate.}$$

In geometric terms, we want to shrink or stretch the tolerance matrix \mathbf{M} by a factor a so that we find the matrix of the same shape and orientation that gives:

$P(\mathbf{X}'a\mathbf{M}\mathbf{X} \leq 1) = \gamma$ or, equivalently:

$$P(\mathbf{X}'a\mathbf{M}\mathbf{X} \leq 1) = P\left(\mathbf{X}'\mathbf{M}\mathbf{X} \leq \frac{1}{a}\right) = P(\mathbf{X}'\mathbf{M}\mathbf{X} \leq c^2) = \gamma$$

Where $c^2 = 1/a$

In order to more easily find c , we can equate the quadratic form $\mathbf{X}'\mathbf{M}\mathbf{X}$ to a linear combination of independent chi-square variables (as the distribution of the latter has been amply discussed in the past in the context of “coverage problems”, as discussed in the *Literature review* section of the present). To accomplish this goal, we apply a series of three transformations of variables. While these three transformations could have been accomplished in a single, albeit more complex, transformation, we present them here in a step-by-step fashion to facilitate understanding.

As a first step, we set $\mathbf{U} = \mathbf{M}^{1/2}\mathbf{X}$.

\mathbf{U} is a linear transformation of a multivariate normal random variable; it is well known that \mathbf{U} itself is also multivariate normal: $\mathbf{U} \sim N_3(0, \Sigma_{\mathbf{u}})$, where $\Sigma_{\mathbf{u}} = \mathbf{M}^{1/2}\Sigma_{\mathbf{X}}\mathbf{M}^{1/2}$.

Because $\mathbf{X}'\mathbf{M}\mathbf{X} = \mathbf{X}'\mathbf{M}^{1/2}\mathbf{M}^{1/2}\mathbf{X} = \mathbf{U}'\mathbf{U}$, $P(\mathbf{X}'\mathbf{M}\mathbf{X} \leq c^2) = P(\mathbf{U}'\mathbf{U} \leq c^2)$

$\Sigma_{\mathbf{u}}$ is a symmetric positive definite matrix and can be decomposed as follows (Johnson and Wichern (2002, pp. 66-67)): $\Sigma_{\mathbf{u}} = \mathbf{P}_{\mathbf{u}}\mathbf{D}_{\mathbf{u}}\mathbf{P}'_{\mathbf{u}}$

where $\mathbf{D}_{\mathbf{u}}$ is a diagonal matrix containing the eigenvalues of $\Sigma_{\mathbf{u}}$:

$$\mathbf{D}_{\mathbf{u}} = \begin{bmatrix} \lambda_{u_1} & 0 & 0 \\ 0 & \lambda_{u_2} & 0 \\ 0 & 0 & \lambda_{u_3} \end{bmatrix}$$

Where $\lambda_{u_1}, \lambda_{u_2}$ and λ_{u_3} are the eigenvalues of the matrix Σ_u and $\lambda_{u_1} \geq \lambda_{u_2} \geq \lambda_{u_3}$

and $\mathbf{P}_u = [\mathbf{e}_{u_1}, \mathbf{e}_{u_2}, \mathbf{e}_{u_3}]$ contains the corresponding orthonormal eigenvectors; we should note that $\mathbf{P}'_u \mathbf{P}_u = \mathbf{I}$.

In a second transformation, we set $\mathbf{V} = \mathbf{P}'_u \mathbf{U}$.

The variance-covariance matrix of \mathbf{V} is:

$$\Sigma_v = \mathbf{P}'_u \Sigma_u \mathbf{P}_u = \mathbf{P}'_u \mathbf{P}_u \mathbf{D}_u \mathbf{P}'_u \mathbf{P}_u = \mathbf{I} \mathbf{D}_u \mathbf{I} = \mathbf{D}_u.$$

That is, $\mathbf{V} \sim N_3(0, \mathbf{D}_u)$.

We then finally have the equation: $\mathbf{U}'\mathbf{U} = \mathbf{V}'\mathbf{P}'_u^{-1}\mathbf{P}'_u^{-1}\mathbf{V} = \mathbf{V}'\mathbf{V}$.

Since we are here discussing the tri-variate case,

$$\mathbf{X}'\mathbf{M}\mathbf{X} = \mathbf{U}'\mathbf{U} = \mathbf{V}'\mathbf{V} = V_1^2 + V_2^2 + V_3^2$$

Since V_1, V_2 and V_3 are normal variables with variance, respectively, $\lambda_{u_1}, \lambda_{u_2}$ and λ_{u_3} , we can equate: $V_1^2 + V_2^2 + V_3^2 = \lambda_{u_1} Y_1^2 + \lambda_{u_2} Y_2^2 + \lambda_{u_3} Y_3^2$, where Y_1, Y_2 and Y_3 are independent standard normal random variables.

That is, we have equated $\mathbf{X}'\mathbf{M}\mathbf{X}$ to a weighted sum of independent chi-square variables, each with one degree of freedom, where the weights are the eigenvalues of the matrix $\Sigma_u = \mathbf{M}^{1/2} \Sigma_v \mathbf{M}^{1/2}$:

$$P(\mathbf{X}'\mathbf{M}\mathbf{X} \leq c^2) = P(\mathbf{U}'\mathbf{U} \leq c^2) = P(V_1^2 + V_2^2 + V_3^2 \leq c^2) = P(\lambda_{u_1} Y_1^2 + \lambda_{u_2} Y_2^2 + \lambda_{u_3} Y_3^2 \leq c^2) = \gamma$$

After briefly discussing the geometry of the above transformations, we will discuss how the proposed process capability index reduces to c .

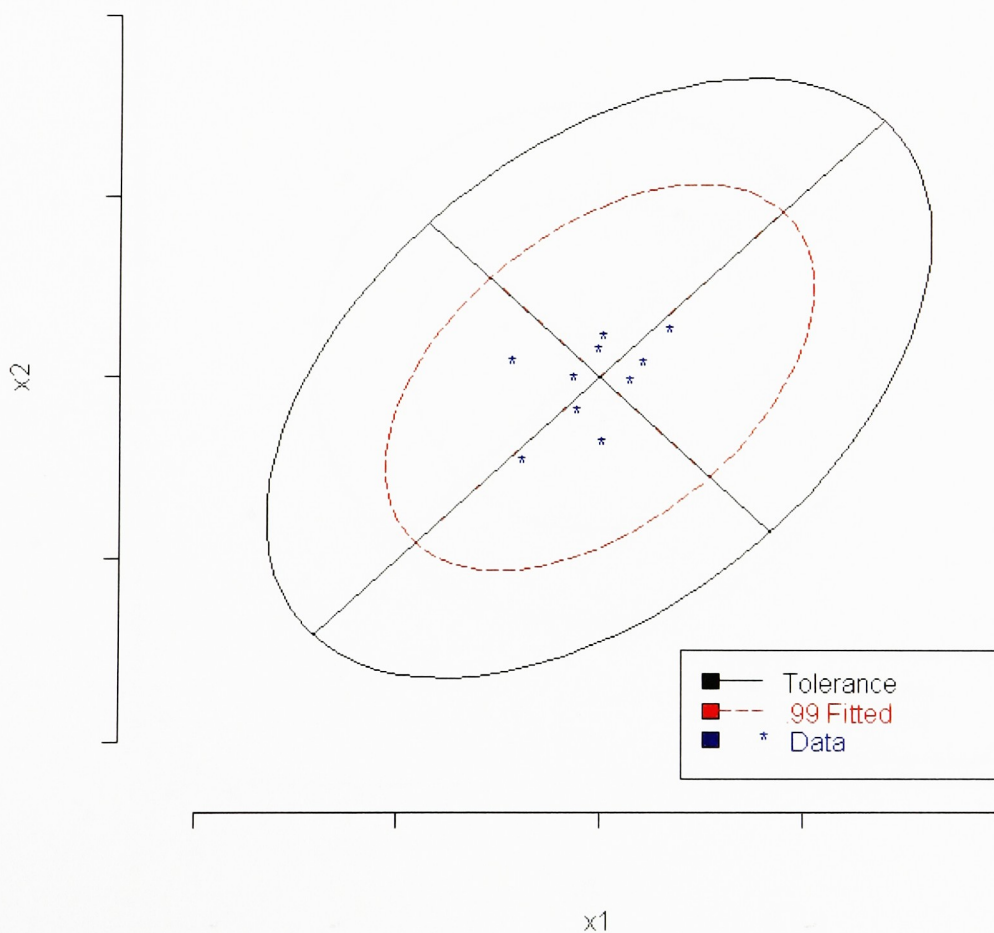
A geometric interpretation of the procedure presented

We have presented the above as three consecutive steps in order to simplify understanding of the procedure. The three steps taken can be easily explained when looked at sequentially and with a geometrical interpretation. Figure 6, Figure 7 and Figure 8, on the following pages, offer a graphical representation of the process.

Please note, we have assumed previously that our measurements follow a multivariate normal distribution, centered at zero; that is, $\mathbf{X} \sim N_3(\mathbf{0}, \Sigma_x)$.

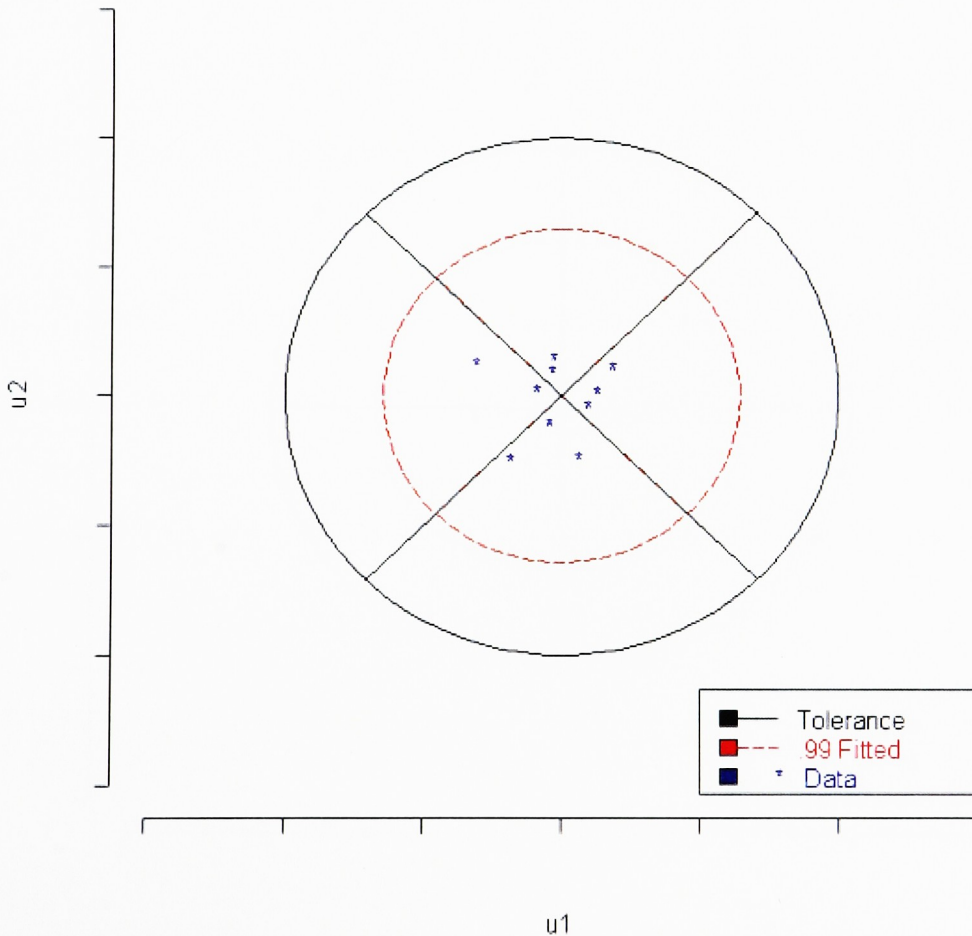
- Step 1: Please refer to Figure 6. Our starting point is the equation of the tolerance ellipsoid, which we can describe by a sequence of points $\{\mathbf{x} : \mathbf{x}'\mathbf{M}\mathbf{x} = 1\}$. A second ellipsoid, with the same shape and orientation, provides a predetermined capture rate and can be described by the set of random variables $\{\mathbf{X} : \mathbf{X}'\mathbf{M}\mathbf{X} \leq c^2\}$. The two ellipsoids have the same shape, orientation and centroid; the two ellipsoids differ in scale (set by the parameter c).

Figure 6. Tolerance, data and fitted ellipse.



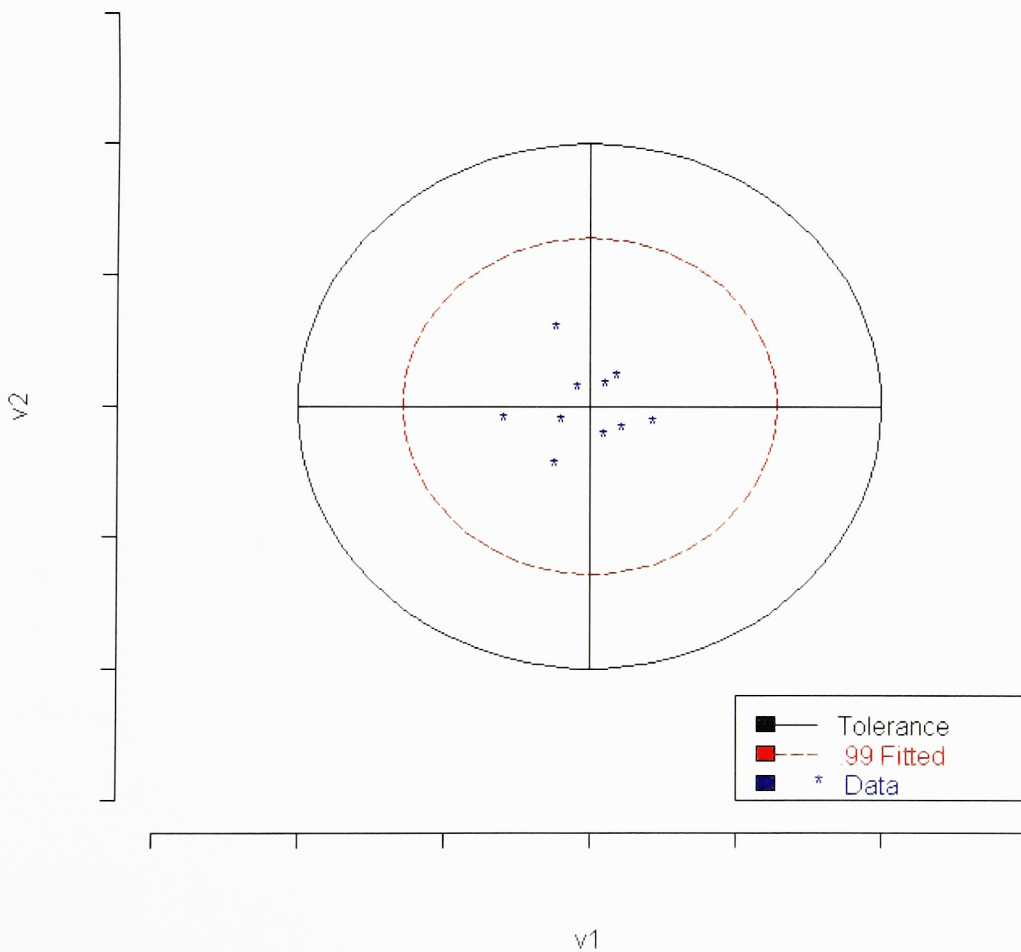
- Step 2: Please refer to Figure 7. The first transformation, $\mathbf{U} = \mathbf{M}^{1/2} \mathbf{X}$, has the effect of shrinking both the tolerance and data ellipsoids along the directions of maximum variability (axes of the tolerance ellipsoid). Both ellipsoids reduce to spheroids; the tolerance ellipsoid can be described by a set of points $\{\mathbf{u} : \mathbf{u}'\mathbf{u} = 1\}$, while the fitted ellipsoid can be described by a set of random variables $\{\mathbf{U} : \mathbf{U}'\mathbf{U} \leq c^2\}$.

Figure 7. Transformation to “U-space”.



- Step 3: Please refer to Figure 8. The second transformation, $\mathbf{V} = \mathbf{P}'_u \mathbf{U}$, rotates both the tolerance and fitted regions. The resulting spheroids have their axis aligned with the coordinate systems. Both ellipsoids reduce to spheroids; the tolerance ellipsoid can be described by a set of points $\{\mathbf{v} : \mathbf{v}'\mathbf{v} = 1\}$, while the fitted ellipsoid can be described by a set of random variables $\{\mathbf{V} : \mathbf{V}'\mathbf{V} \leq c^2\}$.

Figure 8. Transformation to “V-space”.



Estimating c and calculating the multivariate process capability index.

As discussed in the literature review section, various methods and algorithms have been proposed in the past to solve:

$P(\lambda_{u_1} Y_1^2 + \lambda_{u_2} Y_2^2 + \lambda_{u_3} Y_3^2 \leq c^2) = \gamma$, where Y_1 , Y_2 and Y_3 are independent standard normal random variables.

In *Appendix I* we use two algorithms to solve the above equation. The first estimates γ given the eigenvalues λ_{u_1} , λ_{u_2} and λ_{u_3} and the parameter c^2 ; the second algorithm estimates c^2 given the eigenvalues λ_{u_1} , λ_{u_2} and λ_{u_3} and the parameter γ .

The inequality in $P(\lambda_{u_1} Y_1^2 + \lambda_{u_2} Y_2^2 + \lambda_{u_3} Y_3^2 \leq c^2) = \gamma$ is overparametrized. An often used reparametrization employed, for example, in the tables compiled by Marsiglia (1960), leads to: $P(Y_1^2 + r_1 Y_2^2 + r_2 Y_3^2 \leq r_3) = \gamma$

Where

$$r_1 = \lambda_{u_2} / \lambda_{u_1}$$

$$r_2 = \lambda_{u_3} / \lambda_{u_1}$$

$$r_3 = c^2 / \lambda_{u_2}$$

We will continue to use the overparametrized version of the equation in the present discussion.

Once we have \mathbf{M} and c , we can proceed in estimating our summary measure of variability and computing the capability index as follows. Geometrically, as discussed by Johnson and Wichern (2002, pp. 65-66), the three-dimensional fitted ellipsoid can be determined by the three axes, whose orientation is described by the eigenvectors \mathbf{e}_i of the matrix \mathbf{M} and whose half length in the \mathbf{e}_i direction is equal to $c/\sqrt{\lambda_i}$, where λ_i is the i^{th} corresponding eigenvalue of the matrix \mathbf{M} .

In the spherical case, we have $\lambda_1 = \lambda_2 = \lambda_3 = \lambda$. The diameter of the sphere can be calculated as $d = 2c/\sqrt{\lambda}$.

For the purposes of calculating the capability index, we calculate the diameter of the tolerance sphere: $d_{tol} = 2/\sqrt{\lambda}$.

The process capability index, defined as the ratio between the diameter of the “fitted” sphere and the diameter of the tolerance sphere, reduces to:

$$\frac{d}{d_{tol}} = \frac{2c/\sqrt{\lambda}}{2/\sqrt{\lambda}} = c$$

In the ellipsoidal case, we calculate the length of the major axis of the ellipsoid, of the same shape and orientation as the tolerance ellipsoid that provides a pre-determined capture rate γ . Our process capability index will then be the ratio of the major axis of this ellipsoid to the major axis of the tolerance ellipsoid. Clearly, for the purposes of developing a process capability index, the ratio of the major axes will be equal to the ratio of e.g. the minor axes, because the shapes of the ellipsoids are identical.

The length of the major axis of the fitted ellipsoid will be equal to $2c/\sqrt{\lambda_{\min}}$ where $\lambda_{\min} = \min(\lambda_1, \lambda_2, \lambda_3)$. Please note, that the major axis of the ellipse is associated with the smallest eigenvalues of the matrix \mathbf{M} – as the length of each axis is inversely related to the size of the eigenvalues of \mathbf{M} . The length of the major axes of the tolerance ellipsoid will be equal to: $2/\sqrt{\lambda_{\min}}$, so the process capability index is, again, c .

The process capability index, defined as the ratio between the length of the major axis of the “fitted” spheroid and the length of the major axis of the tolerance ellipsoid, reduces to

$$\frac{2c/\sqrt{\lambda_{\max}}}{2/\sqrt{\lambda_{\max}}} = c$$

The use of c as a scale factor allows for quick and intuitive comparisons. So, for example, if $c = 0.1$, we would conclude that the amount of tolerance “used” by the data - or by the particular variance component studied - is 10 percent. This also allows for comparisons of variance components.

Estimating \mathbf{M}

In some applications, the users may not be given a matrix \mathbf{M} that describes the size and orientation of the tolerance region. Rather, a set of acceptable observations may be provided, from which the user has to derive an equation describing the tolerance region. A similar approach was used in the field of color science to derive a series of equations describing tolerance regions whose size and orientation vary according to the position in color space of the measured sample.

We define \mathbf{t}_i as the vector of length 3 containing the measurements of the i^{th} observations.

If we consider a set of data points describing the entire acceptable tolerance region, define

Σ_{tol} as the sample variance-covariance matrix associated with this set of data points.

We then proceed by finding the value $c_{scale,i}^2 = \mathbf{t}_i' \Sigma_{\text{tol}}^{-1} \mathbf{t}_i$ for every observation i .

We define $c_{scale,max}^2 = \max(c_{scale,i}^2)$. We then define \mathbf{M} as: $\mathbf{M} = \frac{1}{c_{scale,max}^2} \Sigma_{\text{tol}}^{-1}$.

Extensions to p dimensions

We present our method in the three-dimensional case, but the argument applies equally well to the p-dimensional case.

With spherical tolerances, our summary measure would be the diameter of the p-dimensional spheroid that leads to a pre-determined capture rate.

With ellipsoidal tolerances, our summary measure would be the length of the major axis of the ellipsoid (of equal shape and orientation to the tolerance ellipsoid) that leads to a pre-determined capture rate.

When fitting this ellipsoid, we would use a similar set of equations:

$$P(\mathbf{X}'\mathbf{M}\mathbf{X} \leq c^2) = P(\mathbf{U}'\mathbf{U} \leq c^2) = P\left(\sum_p \lambda_{u_p} Y_p^2 \leq c^2\right).$$

With either spherical or ellipsoidal tolerances, c can be interpreted as estimating the fraction of tolerance “used” by the component of variance of interest.

In practice, the main use of this is in the two-dimensional case, extending the result of Voelkel (2003).

Application: analysis of color metrics

We present in the following section various applications of the proposed process capability index, in the context of color metrics. Our process capability index is presented within the framework of the CIE_{94} (Berns (2002, pp. 72-74)) standard for color measurements. In the present section, we briefly summarize the most relevant CIE_{94} concepts and how they reflect on the application of our process capability index.

One common coordinate system for reporting color data, and the format in which the datasets were made available to us, is the CIELAB coordinate system (Berns (2002), pp. 72). Briefly, CIELAB can be described as a rectangular coordinate system with axes labeled L^* , a^* and b^* . The magnitude of the L^* coordinate describes the amount of lightness, that of a^* refers to the amount of redness-greenness while that of b^* refers to the amount of yellowness-blueness. “CIE” stands for Commission Internationale de l’Eclairages - an international body of color scientists - while “LAB” refers to the L^* , a^* and b^* coordinate system. Every measurement can then be described, within the CIELAB measurement system, by a vector $\mathbf{v} = (L^* \ a^* \ b^*)'$.

Despite the common use of CIELAB in reporting data, CIE_{94} defines color tolerances within a different coordinate system, defined simply as “lightness-chroma-hue”, with axes labeled L^* , C_{ab}^* , H_{ab}^* .

CIE_{94} offers an equation to estimate the size of the acceptable tolerance region for color differences (Berns (2002, pg. 72)). While this above equation was developed to estimate the

size of a tolerance region around a particular “standard”, we have applied a slight modification to the formulas supplied, in order to compute color differences around the mean. We define:

$$\Delta E_{94} = \left(\frac{\Delta L^*}{k_L S_L} \right)^2 + \left(\frac{\Delta C_{ab}^*}{k_C S_C} \right)^2 + \left(\frac{\Delta H_{ab}^*}{k_H S_H} \right)^2, \text{ where:}$$

$$S_L = 1$$

$$S_C = 1 + 0.045 \overline{C}_{ab}^*$$

$$S_H = 1 + 0.015 \overline{C}_{ab}^*$$

$$k_L = k_H = k_C = 1 \text{ for reference conditions}$$

Similarly, with slight modifications to the standard formulas (Berns (2002, pp. 72), Stokes (1992), Seve (1996)):

$$\Delta L^* = L_{batch}^* - \overline{L}^*$$

$$\Delta C_{ab}^* = \left((a_{batch}^*)^2 + (b_{batch}^*)^2 \right)^{1/2} - \left((\overline{a}^*)^2 + (\overline{b}^*)^2 \right)^{1/2}$$

$$\Delta H_{ab}^* = \frac{a_{batch}^* \overline{b}^* - \overline{a}^* b_{batch}^*}{\left[0.5 (C_{ab, batch}^* \overline{C}_{ab}^* + a_{batch}^* \overline{a}^* + b_{batch}^* \overline{b}^*) \right]^{1/2}}$$

Finally, to obtain an estimate of our tolerance region, given a certain position in the a^*, b^* color space, which reflects in the \overline{C}_{ab}^* factor, we have to set a maximum acceptable “overall color difference”, as measured by ΔE_{94} . For the purposes of the present example, we will set $\Delta E_{94} = 1$, a value commonly used in industrial application, although the exact value

will depend on the particular application studied. In an applied situation, the value of ΔE_{94} will be established by the user.

The region containing acceptable observation can then be described as:

$$\left\{ \mathbf{T} : \left(\frac{\Delta L^*}{k_L S_L} \right)^2 + \left(\frac{\Delta C_{ab}^*}{k_C S_C} \right)^2 + \left(\frac{\Delta H_{ab}^*}{k_H S_H} \right)^2 \leq 1 \right\}$$

Given a set of L^* , a^* and b^* measurements, we are then able to both transform the data and derive an equation for the tolerance region in ΔL^* , ΔC_{ab}^* , ΔH_{ab}^* space.

The size and orientation of the tolerance region can be described by a diagonal matrix:

$$\mathbf{M} = \begin{bmatrix} 1 & 0 & 0 \\ 0 & 1/S_C^2 & 0 \\ 0 & 0 & 1/S_H^2 \end{bmatrix}$$

We should observe that the tolerance ellipsoid axes defined by the CIE_{94} standard, are aligned with the ΔL^* , ΔC_{ab}^* , ΔH_{ab}^* coordinate system.

To estimate the scale factor c for a particular variance component, we need to estimate the eigenvalues of the matrix $\Sigma_u = \mathbf{M}^{1/2} \Sigma_x \mathbf{M}^{1/2}$, which in turn requires an estimate of Σ_x .

In our simplest scenario (one operator, using one gauge to take n measurements on a part),

we could model each reading $\mathbf{X}_i = (\Delta L_i^* \ \Delta C_{ab}^* \ \Delta H_{ab}^*)'$ as follows:

$\mathbf{X}_i = \boldsymbol{\mu} + \boldsymbol{\varepsilon}_i$, with:

$$\boldsymbol{\mu} = (0 \ 0 \ 0)'$$

$$\boldsymbol{\varepsilon}_i \sim N_3(\mathbf{0}, \boldsymbol{\Sigma}_x)$$

We can easily estimate $\boldsymbol{\Sigma}_x$ as

$$\hat{\boldsymbol{\Sigma}}_x = \begin{pmatrix} \text{Var}(\Delta L^*) & \text{Cov}(\Delta L^*, \Delta C_{ab}^*) & \text{Cov}(\Delta L^*, \Delta H_{ab}^*) \\ \text{Cov}(\Delta C_{ab}^*, \Delta L^*) & \text{Var}(\Delta C_{ab}^*) & \text{Cov}(\Delta C_{ab}^*, \Delta H_{ab}^*) \\ \text{Cov}(\Delta H_{ab}^*, \Delta L^*) & \text{Cov}(\Delta H_{ab}^*, \Delta C_{ab}^*) & \text{Var}(\Delta H_{ab}^*) \end{pmatrix}$$

Once we have obtained our estimate of $\boldsymbol{\Sigma}_x$ as described above, we can proceed by

finding $\hat{\boldsymbol{\Sigma}}_u = \mathbf{M}^{1/2} \hat{\boldsymbol{\Sigma}}_x \mathbf{M}^{1/2}$.

We then calculate the eigenvalues $\hat{\lambda}_{u_1}, \hat{\lambda}_{u_2}, \hat{\lambda}_{u_3}$ of the matrix $\hat{\boldsymbol{\Sigma}}_u$ and use the latter in

estimating c in $P(\hat{\lambda}_{u_1} Y_1^2 + \hat{\lambda}_{u_2} Y_2^2 + \hat{\lambda}_{u_3} Y_3^2 \leq c^2) = \gamma$.

To find c for a given set of eigenvalues $\lambda_{u_1}, \lambda_{u_2}, \lambda_{u_3}$ and a capture rate γ , we proposed an algorithm in *Appendix 1*, which is an adaptation of the *Ruben* algorithm presented by Farebrother (1984).

In more complex cases, such as a typical gauge R&R study, we are interested in the estimation of components of variance. In typical applications, we can assume that the variation of a process can be subset into short, medium and long term components. For example, we could assume that we could model each reading $\mathbf{x}_{ijk} = \left(\Delta L_{ijk}^* \quad \Delta C_{ab_{ijk}}^* \quad \Delta H_{ab_{ijk}}^* \right)'$ as follows:

$$\mathbf{x}_{ijk} = \boldsymbol{\mu} + \mathbf{s}_i + \mathbf{m}_j + \mathbf{l}_k, \text{ with:}$$

$$\boldsymbol{\mu} = (0 \ 0 \ 0)'$$

$$\mathbf{s}_i \sim \text{MVN}(0, \boldsymbol{\Sigma}_s)$$

$$\mathbf{m}_j \sim \text{MVN}(0, \boldsymbol{\Sigma}_m)$$

$$\mathbf{l}_k \sim \text{MVN}(0, \boldsymbol{\Sigma}_l)$$

Please note that the total error term $\boldsymbol{\Sigma}_x$ is equal to the sum of the short, medium and long term components: $\boldsymbol{\Sigma}_x = \boldsymbol{\Sigma}_s + \boldsymbol{\Sigma}_m + \boldsymbol{\Sigma}_l$.

Multivariate ANOVA techniques and, in particular, the so called “method of moments” (Montgomery (2001, pp 512-549), Jobson (1999), Rencher(2002)) can be employed to obtain $\hat{\Sigma}_s$, $\hat{\Sigma}_m$ and $\hat{\Sigma}_1$. We can then calculate:

$$\hat{\Sigma}_{u,s} = \mathbf{M}^{1/2} \hat{\Sigma}_s \mathbf{M}^{1/2}$$

$$\hat{\Sigma}_{u,m} = \mathbf{M}^{1/2} \hat{\Sigma}_m \mathbf{M}^{1/2}$$

$$\hat{\Sigma}_{u,1} = \mathbf{M}^{1/2} \hat{\Sigma}_1 \mathbf{M}^{1/2}$$

$$\hat{\Sigma}_u = \mathbf{M}^{1/2} \hat{\Sigma}_x \mathbf{M}^{1/2}$$

We can then obtain the four sets of eigenvalues to obtain estimates of $c, c_{st}, c_{mt}, c_{lt}$.

These four estimates would correspond to common summaries of the measurement systems.

For example, c_{st} would be an estimate of short term repeatability.

In the one-dimensional case, we can observe that: $c^2 = c_{st}^2 + c_{mt}^2 + c_{lt}^2$. Voelkel (2003) proved that, in the two-dimensional case, $c^2 \leq c_{st}^2 + c_{mt}^2 + c_{lt}^2$ - the case for perfect additivity only holds when all of the components of variance are oriented in the same direction (that is, the estimated variance-covariance matrices all have the same eigenvectors). The same concept applies to three or more dimensions: $c^2 \leq c_{st}^2 + c_{mt}^2 + c_{lt}^2$, with the equality holding only when all components of variance have the same spatial orientation.

In the same way the method of moments applied to univariate cases can result in negative component of variance estimates, in multivariate settings the method of moments can result in estimated matrices that are not non-negative definite.

From our examples, we observed that this problem tends to most often manifest itself, in multivariate settings, when most of the variance is aligned with one dimension. For example, we encountered this problem when estimating variance components in our third example (the long-term cyan data).

When the estimated components of variance are not non-negative definite matrices, we used the Calvin-Dykstra algorithm (Calvin and Dykstra (1991)). Other possible remedial measures are described by Calvin and Dykstra (1991).

Applications

We present here three different examples, all relative to estimation of variance (and components of variance) of color metrics.

1. An estimation of inter-instrument reproducibility and of the related components of variance (short terms and medium term) and possible interactions (instrument*medium-term), based on measurements on a white sample.
2. A comparison of the components of variance (short-term and medium-term) of measurements obtained with 12 different instruments, based on measurements on a white sample.

3. A comparison of the long-term and medium-term variability components of 12 instruments used to measure a cyan tile.

The instruments used in the three examples are of three different kinds: handheld spheres, benchtop spheres and handheld bidirectional. The instruments were labeled as follows:

Table 1. Instrument types.

Instrument	Type
A	Handheld Sphere
B	Handheld Sphere
C	Handheld Sphere
D	Handheld Sphere
E	Benchtop Sphere
F	Benchtop Sphere
G	Benchtop Sphere
H	Benchtop Sphere
I	Handheld Bidirectional
J	Handheld Bidirectional
K	Handheld Bidirectional
L	Handheld Bidirectional

Two pairs of identical models were included in the experiment: A and B, K and L.

The experiments were conducted under the assumption that no operator effects would be significant. Under this assumption, no data on operators has been collected and the assumption itself could not be tested.

The capture rate γ for the data-fitted ellipsoids has been set in these examples at .99.

The data was made available to us in the L^* , a^* and b^* metrics. We converted to ΔL^* , ΔC_{ab}^* , ΔH_{ab}^* space using the formulas discussed in the previous section.

After converting the data to ΔL^* , ΔC_{ab}^* , ΔH_{ab}^* space, we proceeded by verifying that the data did meet our assumptions – that is, that the data is multivariate normal and that no trends over time are present. Our technique requires also that the mean of each univariate distribution is zero - given that ΔL^* , ΔC_{ab}^* , ΔH_{ab}^* are essentially differences from the mean value, they are necessarily centered at zero.

We first checked for independence over time (that is, for a lack of time-related trends or measurement drift). No formal tests were employed – rather, the data was plotted versus the order of observation and visually inspected for trends.

In order to verify the normality assumption, we utilized four univariate tests (Shapiro-Wilkins (Shapiro and Wilkins (1965)), Kolmogorov-Smirnov, Cramer and Anderson Darling (Ryan and Joiner (1976))) to check for departures from normality in the univariate data distributions. Finally, we employed the Mardia tests for Skeweness and Kurtosis (Mardia (1980)) and the Henze Zirkler T-test for normality (Henze and Zirkler (1990)) to check for multivariate departures. We used normal probability plots and chi-square Q-Q plots (Chambers, Cleveland, Kleiner and Tukey (1983)) to assess univariate and multivariate normality departures. The procedure applied is exemplified for one instrument in *Appendix 3*. Overall, we were satisfied with the results of such tests and concluded that the data did not present problematic departures from our assumptions.

Example 1

The dataset used in this first example consisted of 10 measurements taken every hour, for 8 hours, on each of 12 instruments.

We assume that we could model each reading $\mathbf{x}_{ijk} = \left(\Delta L_{ijk}^* \quad \Delta C_{ab,ijk}^* \quad \Delta H_{ab,ijk}^* \right)'$ as follows:

$\mathbf{X}_{ijk} = \boldsymbol{\mu} + \mathbf{m}_i + \mathbf{i}_j + \mathbf{mi}_{ij} + \mathbf{s}_{k(ij)}$, with:

$$\boldsymbol{\mu} = (0 \ 0 \ 0)'$$

$$\mathbf{m}_i \sim N_3(\mathbf{0}, \boldsymbol{\Sigma}_m)$$

$$\mathbf{i}_j \sim N_3(\mathbf{0}, \boldsymbol{\Sigma}_i)$$

$$\mathbf{mi}_{ij} \sim N_3(\mathbf{0}, \boldsymbol{\Sigma}_{mi})$$

$$\mathbf{s}_{k(ij)} \sim N_3(\mathbf{0}, \boldsymbol{\Sigma}_s), \text{ where we define:}$$

$\boldsymbol{\Sigma}_x$ = total variance

$\boldsymbol{\Sigma}_s$ = short-term (within the hour) variance component

$\boldsymbol{\Sigma}_m$ = medium-term (hour-to-hour) variance component

$\boldsymbol{\Sigma}_i$ = instrument variance component

$\boldsymbol{\Sigma}_{mi}$ = instrument – medium term interaction component

Using the CIE_{94} equations, we find that the tolerance matrix associated with a white sample is simply a sphere:

$$\mathbf{M} = \begin{bmatrix} 1 & 0 & 0 \\ 0 & 1 & 0 \\ 0 & 0 & 1 \end{bmatrix}.$$

We report here one of the metrics used in the test for significance of variance components, the p-value associated with the F statistic for Wilks' multivariate test (Johnson and Wichern (2002)). When tested at a 5% significance level, the instrument and the instrument-medium term interaction components of variance were significant, but the medium-term component was not. In our analysis, we retained the MT component of variance, because the higher-level interaction is significant; in order to obtain a meaningful estimate of Σ_m , we applied the Calvin Dykstra algorithm).

Table 2. Significance of variance components, Example 1.

Component	Wilks' p-value
Instrument	0.0000
MT	0.5450
Instrument*MT	0.0000
ST	na

Using the expected mean square table presented in Table 1, we obtained the following estimates for our components of variance:

$$\hat{\Sigma}_x = \begin{pmatrix} .3289 & .0261 & .0077 \\ .0261 & .0541 & -.0234 \\ .0077 & -.0234 & .0257 \end{pmatrix}$$

$$\hat{\Sigma}_s = \begin{pmatrix} .0425 & -.0010 & .0019 \\ -.0010 & .0006 & -.0001 \\ .0019 & -.0001 & .0006 \end{pmatrix}$$

$$\hat{\Sigma}_{mi} = \begin{pmatrix} .1225 & .0096 & .0005 \\ .0096 & .0037 & .0005 \\ .0005 & .0005 & .0005 \end{pmatrix}$$

$$\hat{\Sigma}_m = \begin{pmatrix} .0054 & -.0005 & .0003 \\ -.0005 & .0000 & .0000 \\ .0003 & .0000 & .0000 \end{pmatrix}$$

$$\hat{\Sigma}_i = \begin{pmatrix} .1585 & .0179 & .0050 \\ .0179 & .0498 & -.0238 \\ .0050 & -.0238 & .0246 \end{pmatrix}$$

Table 3. EMS for Example 1.

Source	df	EMS
Instrument	11	$\Sigma_s + 10\Sigma_{im} + 80\Sigma_i$
MT	7	$\Sigma_s + 10\Sigma_{mi} + 120\Sigma_m$
Instrument*MT	77	$\Sigma_s + 10\Sigma_{mi}$
ST	864	Σ_s
Total	959	

Once we obtained the above estimates, we could employ the algorithms presented in *Appendix 1* to calculate our process capability index for each component of variance.

Keeping in mind that, because $\mathbf{M} = \mathbf{I}$,

$$\hat{\Sigma}_u = \mathbf{M}^{1/2} \hat{\Sigma}_x \mathbf{M}^{1/2} = \hat{\Sigma}_x$$

$$\hat{\Sigma}_{u,st} = \mathbf{M}^{1/2} \hat{\Sigma}_{st} \mathbf{M}^{1/2} = \hat{\Sigma}_{st}$$

$$\hat{\Sigma}_{u,instrument*mt} = \mathbf{M}^{1/2} \hat{\Sigma}_{instrument*mt} \mathbf{M}^{1/2} = \hat{\Sigma}_{instrument*mt}$$

$$\hat{\Sigma}_{u,mt} = \mathbf{M}^{1/2} \hat{\Sigma}_{mt} \mathbf{M}^{1/2} = \hat{\Sigma}_{x,mt}$$

$$\hat{\Sigma}_{u,instrumentt} = \mathbf{M}^{1/2} \hat{\Sigma}_{instrumentt} \mathbf{M}^{1/2} = \hat{\Sigma}_{instrumentt}$$

The estimated process capability indices for each component of variance and for the total are presented in Table 4 and plotted in Figure 9.

Table 4. Process capability indices, Example 1.

Component	c^2	c
Instrument	1.17	1.08
MT	0.04	0.19
Inst*MT	0.82	0.91
ST	0.28	0.53
Total	2.29	1.51

Figure 9. Process capability indices, Example 1.

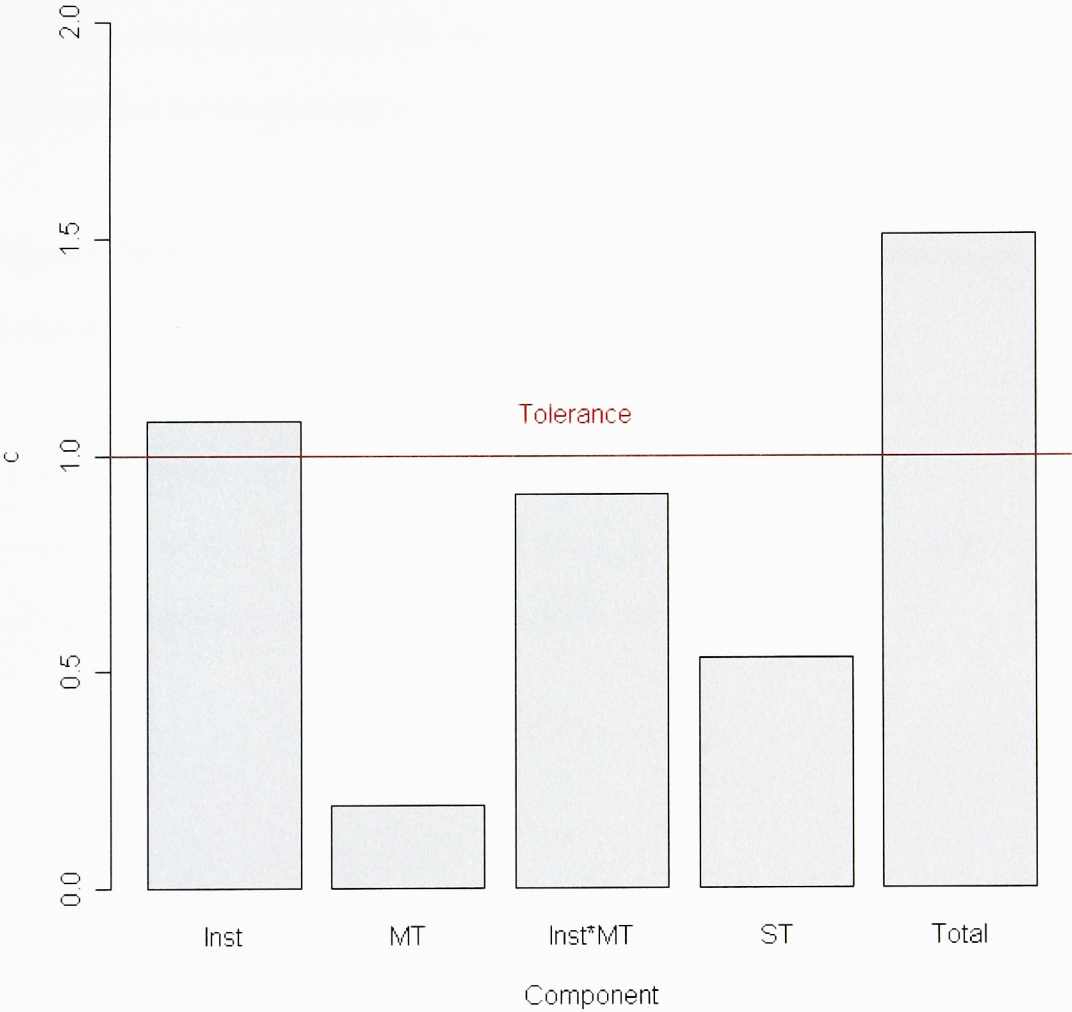


Figure 10 depicts the data points, the tolerance region and the .99 capture region of the same shape and orientation as the tolerance region. In this case, as the c value of 1.54 indicates, the length of the major axis of this fitted region is approximately 1.5 times the length of the major axis of the tolerance region.

Figure 11 depicts the tolerance region and the natural .99 capture ellipsoids relative to each variance component.

Figure 12 depicts the tolerance region and the fitted spheres relative to each variance component. As the c value of 1.08 indicates, the instrument-to-instrument component of variance by itself exceeds the size of the tolerance region.

Figure 10. Data, tolerance and fitted ellipsoid, Example 1.

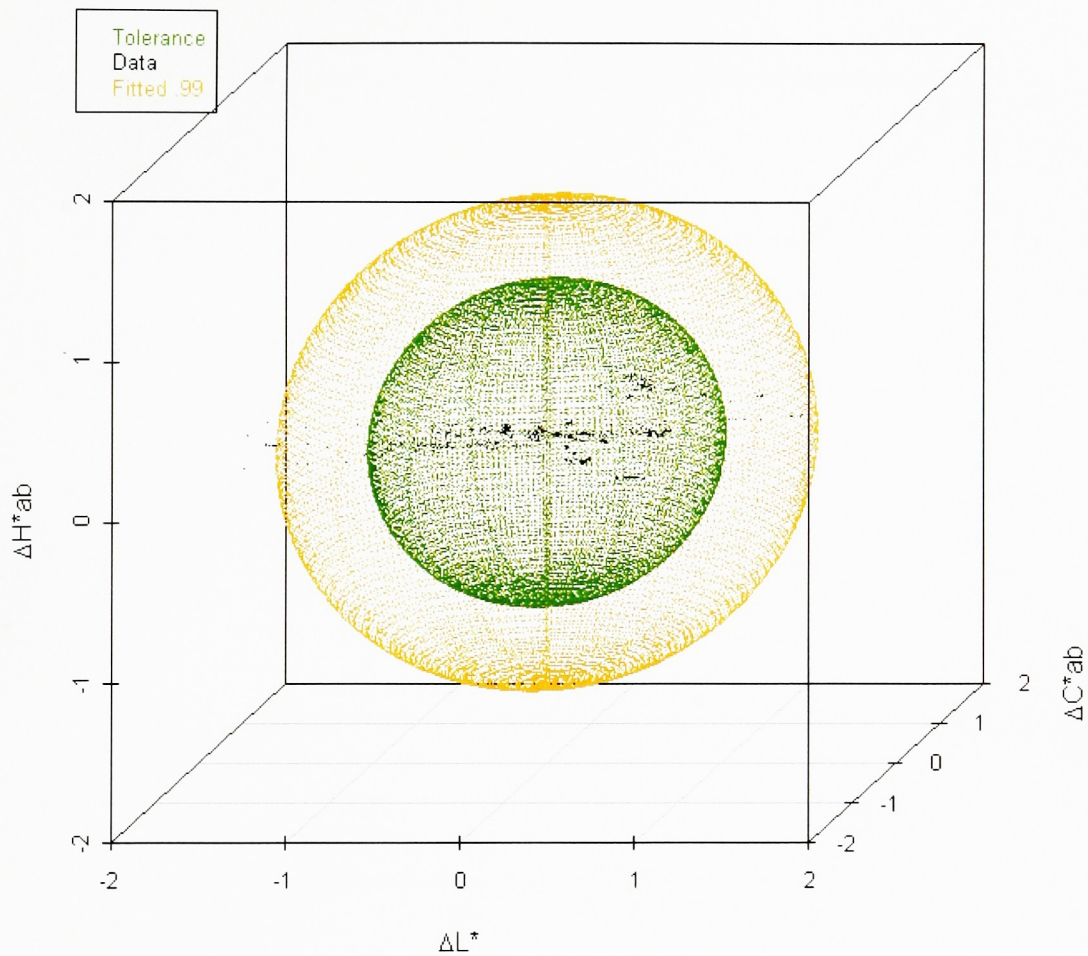


Figure 11. Tolerance and natural .99 capture ellipsoids for each variance component, Example 1.

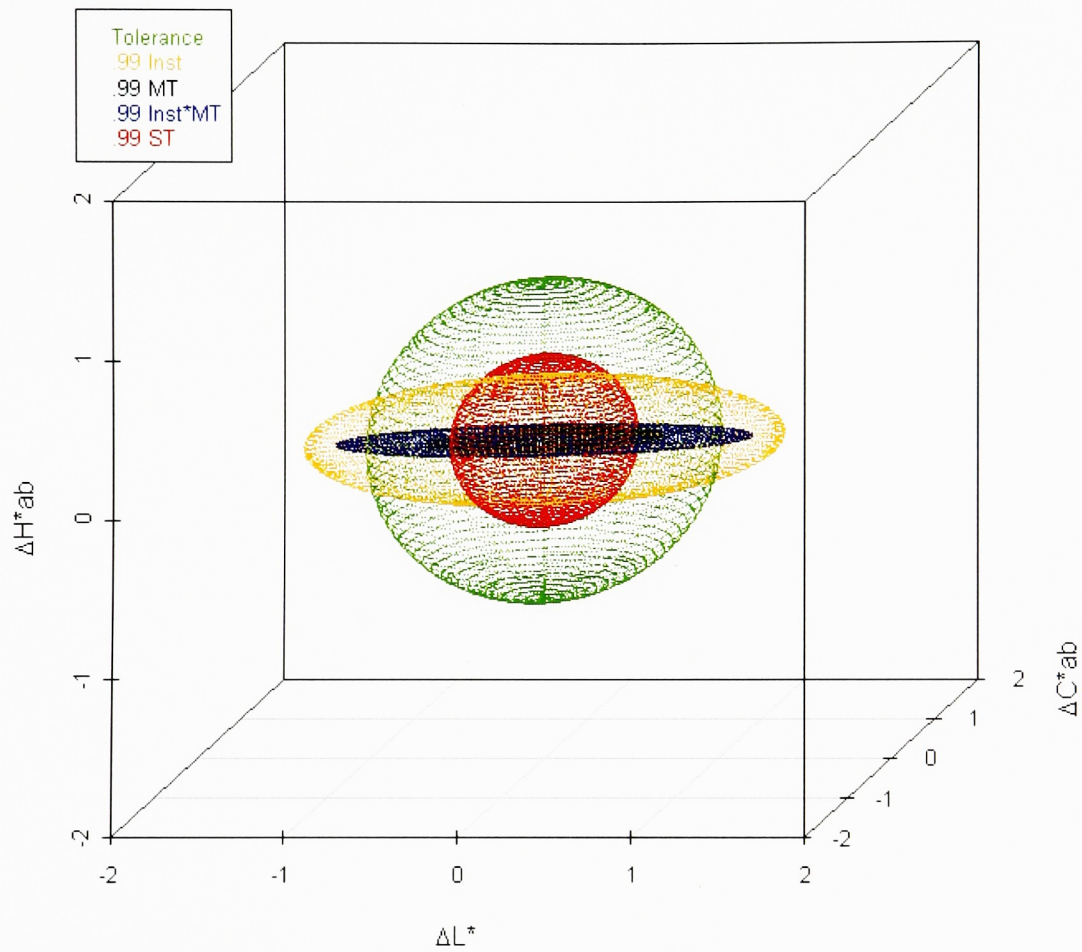
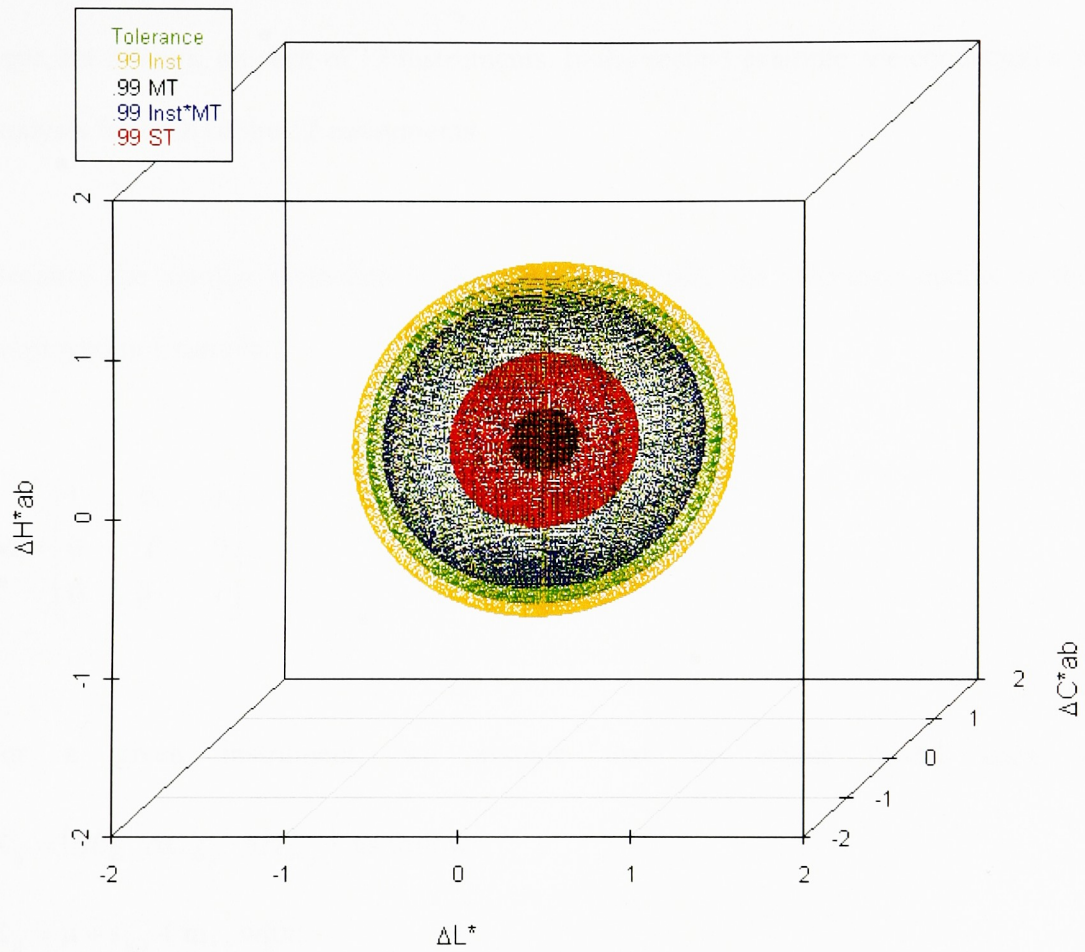


Figure 12. Tolerance and fitted .99 capture spheres for each variance component, Example 1.



Example 2

The dataset used in the first and second example consisted of 10 measurements taken every hour, for 8 hours, on each of 12 instruments. In the second example, we conducted a separate analysis for each of the 12 instruments.

Because the sample measured is the same white tile, the tolerance matrix is the same employed in Example 1:

$$\mathbf{M} = \begin{bmatrix} 1 & 0 & 0 \\ 0 & 1 & 0 \\ 0 & 0 & 1 \end{bmatrix}.$$

For a given instrument, we assume that we could model each reading

$\mathbf{X}_{ij} = (\Delta L_{ijk}^* \quad \Delta C_{ab,ijk}^* \quad \Delta H_{ab,ijk}^*)'$ as follows:

$\mathbf{X}_{ij} = \boldsymbol{\mu} + \mathbf{s}_{i(j)} + \mathbf{m}_j$, with:

$$\boldsymbol{\mu} = (0 \ 0 \ 0)'$$

$$\mathbf{s}_{i(j)} \sim \text{MVN}(\mathbf{0}, \boldsymbol{\Sigma}_s)$$

$$\mathbf{m}_j \sim \text{MVN}(\mathbf{0}, \boldsymbol{\Sigma}_m)$$

We allow for $\boldsymbol{\Sigma}_s$ and $\boldsymbol{\Sigma}_m$ to be estimated separately for each instrument.

We tested for the significance of variance components and obtained estimates for the sum of square and cross product matrices associated with each variance component. Based on the p-value associated with the F statistic for Wilks' multivariate test, all of the tested components of variance were significant at a 5% significance level.

Table 5. EMS, Example 2.

Source	df	EMS
MT	7	$\Sigma_s + 10\Sigma_m$
ST	72	Σ_m
Total	79	

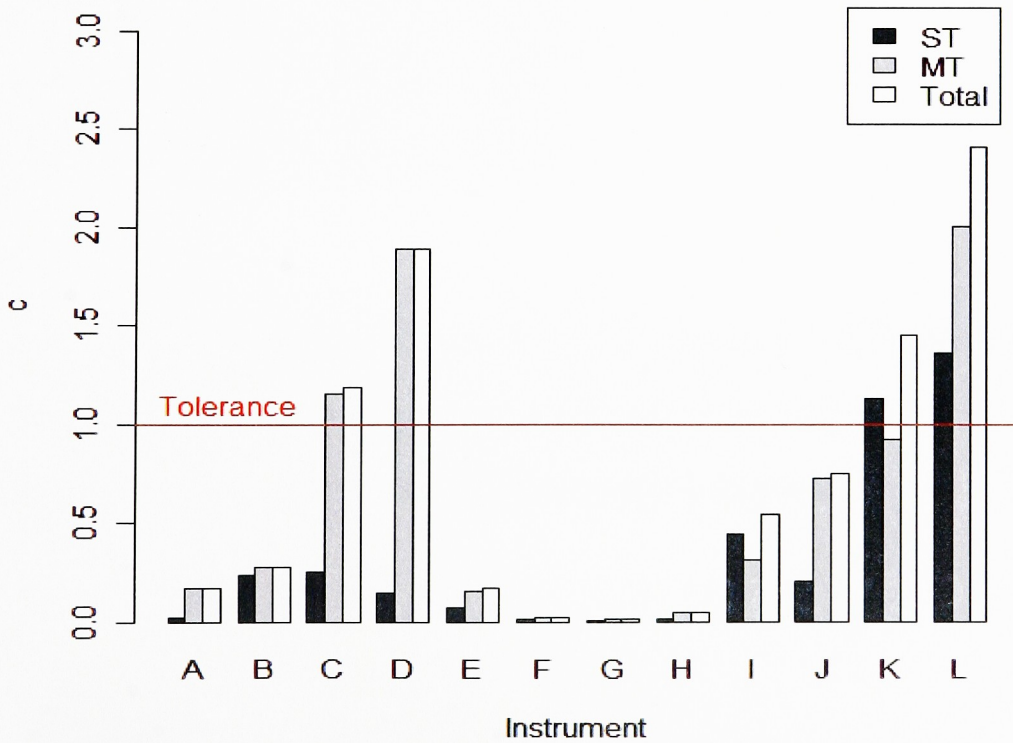
When computing these components-of-variance estimates, we obtained s matrices as components estimates that were not non-negative definite. We employed the Calvin-Dykstra algorithm to obtain new estimates for those components.

Our results, presented in Table 6 and Figure 13, point to dramatic differences in performance across instruments. Instruments C, D, K and L obtained c values larger than one, indicating that a portion of their observations is expected to fall outside of the tolerance region. In instruments C and D this was due to a large medium-term variance component. A similar phenomenon was observed for instruments K and L, but here the short-term component of variance appears considerably larger than for other instruments as well.

Table 6. Process capability indices, Example 2.

Instrument	c^2			c		
	ST	MT	Total	ST	MT	Total
A	0.0006	0.0301	0.0305	0.0237	0.1734	0.1747
B	0.0005	0.0761	0.0766	0.0233	0.2758	0.2767
C	0.0624	1.3390	1.4000	0.2499	1.1572	1.1832
D	0.0211	3.5563	3.5777	0.1454	1.8858	1.8915
E	0.0051	0.0251	0.0302	0.0715	0.1583	0.1737
F	0.0001	0.0006	0.0007	0.0121	0.0239	0.0263
G	0.0001	0.0003	0.0003	0.0073	0.0170	0.0178
H	0.0003	0.0024	0.0026	0.0175	0.0488	0.0511
I	0.2004	0.0955	0.2946	0.4477	0.3090	0.5428
J	0.0400	0.5281	0.5643	0.1999	0.7267	0.7512
K	1.2742	0.8451	2.1176	1.1288	0.9193	1.4552
L	1.8503	4.0083	5.8074	1.3603	2.0021	2.4098

Figure 13. Process capability index, Example 2.



We can also use the concepts presented here to estimate the proportion of points expected to fall within the tolerance region, for each variance component. We do this by solving $P(\lambda_{u_1}y_1^2 + \lambda_{u_2}y_2^2 + \lambda_{u_3}y_3^2 \leq 1) = \gamma$ for γ using the function *Rub* presented in *Appendix 1*.

The expected proportion of observations within tolerance relative to each variance component for each instrument is presented in Table 6.

Table 7. Expected proportion of observation falling within tolerance, Example 2.

Instrument	γ		
	ST	MT	Total
A	~100.0%	~100.0%	~100.0%
B	~100.0%	~100.0%	~100.0%
C	~100.0%	97.4%	96.8%
D	~100.0%	82.8%	82.6%
E	~100.0%	~100.0%	~100.0%
F	~100.0%	~100.0%	~100.0%
G	~100.0%	~100.0%	~100.0%
H	~100.0%	~100.0%	~100.0%
I	~100.0%	~100.0%	~100.0%
J	~100.0%	~100.0%	99.9%
K	97.8%	99.5%	92.3%
L	94.2%	80.1%	71.1%

As an example, we present the results obtained for instrument A in Figure 14 and Figure 15. Figure 14 presents the data points and the tolerance region. Figure 15 depicts the tolerance region and the fitted spheres relative to each variance component.

Figure 14. Data and tolerance region, instrument A, Example 2.

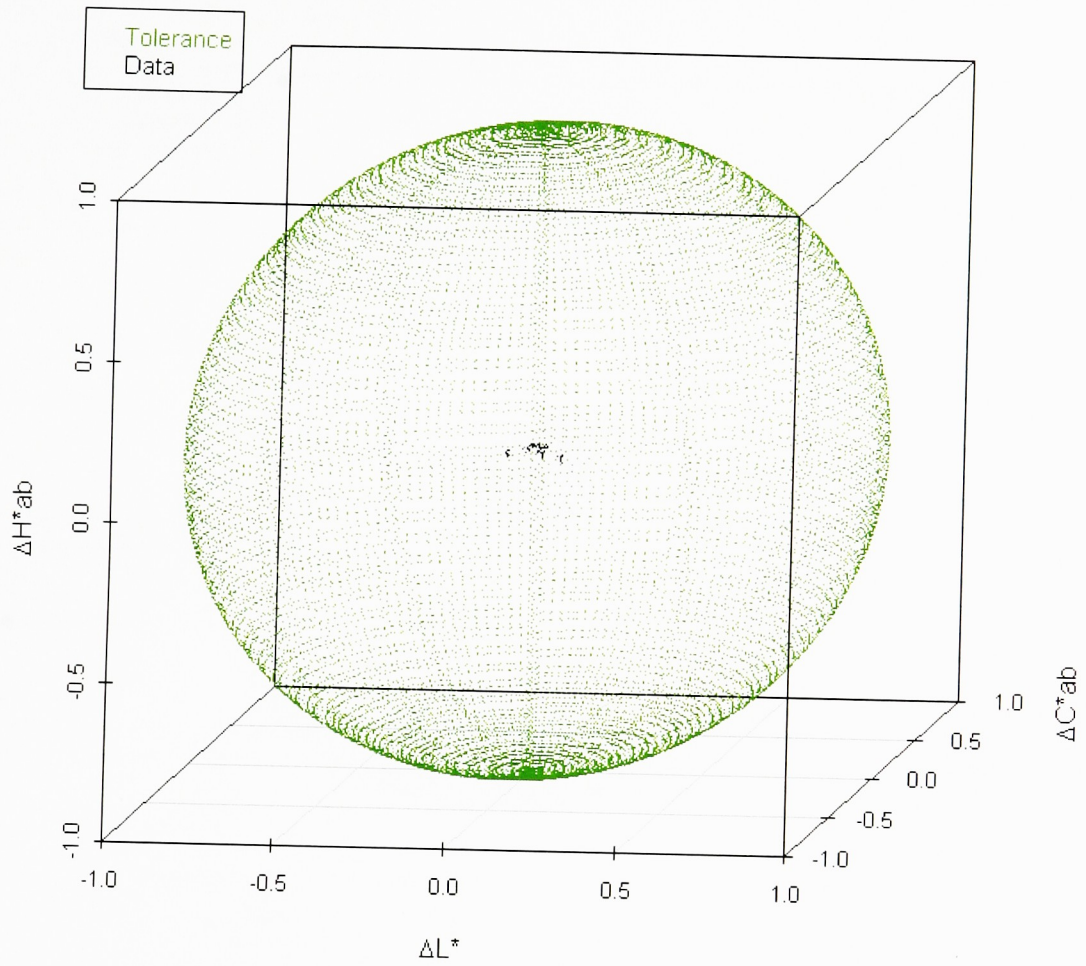
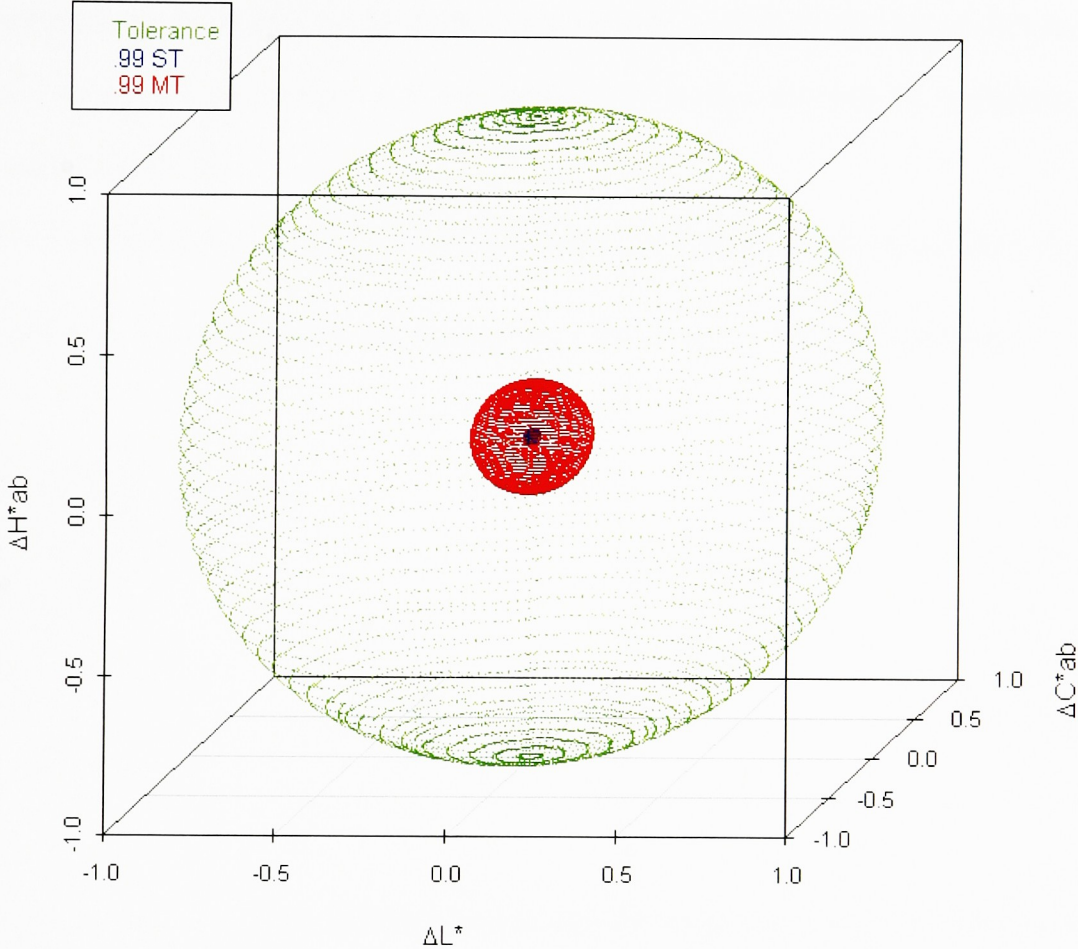


Figure 15. Tolerance region and fitted .99 capture spheres for each variance component, instrument A, Example 2.



Example 3

The dataset used in this example included 12 instruments (labeled A-L), each used to make 2 measurements every day, for 25 days, on a cyan sample. Data for Instrument D was missing for 3 days, data for instrument E was missing for 5 days and data for instrument H was missing for one day.

We conducted a separate analysis for each of the 12 instruments. We assume that, for a given

instrument, we could model each reading $\mathbf{X}_{ij} = \left(\Delta L_{ijk}^* \quad \Delta C_{ab_{ijk}}^* \quad \Delta H_{ab_{ijk}}^* \right)'$ as follows:

$$\mathbf{X}_{ij} = \boldsymbol{\mu} + \mathbf{m}_{i(j)} + \mathbf{I}_j, \text{ with:}$$

$$\boldsymbol{\mu} = (0 \ 0 \ 0)'$$

$$\mathbf{m}_{i(j)} \sim N_3(\mathbf{0}, \boldsymbol{\Sigma}_{mt})$$

$$\mathbf{I}_j \sim N_3(\mathbf{0}, \boldsymbol{\Sigma}_{it})$$

Because we are measuring a different sample than the white used in the first two examples, we have to use the CIE₉₄ equations to determine the size and orientation of the tolerance region.

To obtain the equation of the tolerance matrix, we calculated \bar{a}^* and \bar{b}^* and the related parameters, obtaining the results presented in Table 8.

Table 8. Tolerance region parameters, cyan, Example 3.

Parameter	Value
mean a*	-28.3605
mean b*	-38.4245
mean C*ab	47.7573
$1/SI^2$	1.0000
$1/Sc^2$	3.1491
$1/Sh^2$	1.7164

The resulting tolerance region can then be described by the matrix

$$\mathbf{M} = \begin{bmatrix} 1 & 0 & 0 \\ 0 & 3.14 & 0 \\ 0 & 0 & 1.72 \end{bmatrix}.$$

We tested for the significance of variance components and obtained estimates for the sum of square and cross product matrices associated with each variance component. We used the p-value associated with the F statistic for Wilks' multivariate test to determine which components of variance were not significant; we set the level of significance at 5%. All of the components of variance tested resulted statistically significant, except for the medium-term variance components for instruments A, C and D.

Using the expected mean squares presented in Table 9, we obtained estimates for the variance-covariance matrices associated with each component of variance, for each instrument.

When computing these components-of-variance estimates, we obtained some matrices as components estimates that were not non-negative definite (namely, the estimates of the long term variance-covariance matrices associated with instruments B, F, J, K and L). We employed the Calvin-Dykstra algorithm to obtain new estimates for those components.

Using the algorithm presented in *Appendix 1*, we were then able to compute our process capability indices as shown in Table 10 and in Figure 16.

Table 9. EMS, Example 3.

Source	Df*	EMS
LT	24	$\Sigma_m + 2\Sigma_1$
MT	25	Σ_m
Total	49	

Table 10. Process capability indices, Example 3.

Instrument	c^2			c		
	MT	LT	Total	MT	LT	Total
A	0.1087	0.0000	0.1087	0.3296	0.0000	0.3296
B	0.0603	0.0797	0.1399	0.2456	0.2824	0.3741
C	0.1054	0.0000	0.1054	0.3246	0.0000	0.3246
D	3.4117	0.0000	3.4117	1.8487	0.0000	1.8487
E	0.1930	0.0522	0.2445	0.4393	0.2285	0.4945
F	0.0234	0.0185	0.0411	0.1531	0.1359	0.2028
G	0.0088	0.0450	0.0534	0.0937	0.2120	0.2312
H	0.0026	0.0286	0.0311	0.0508	0.1690	0.1763
I	0.1006	0.0212	0.1134	0.3172	0.1455	0.3367
J	0.1329	0.0852	0.2170	0.3645	0.2920	0.4659
K	0.1117	0.0903	0.2017	0.3342	0.3006	0.4491
L	0.2582	0.0270	0.2683	0.5081	0.1642	0.5180

All of the instruments except for instrument D display repeatability well within tolerance.

The medium term variance component of D, with an associated c value of 1.8, is the only component of variance exceeding tolerance.

Figure 16. Process capability indices, Example 3.

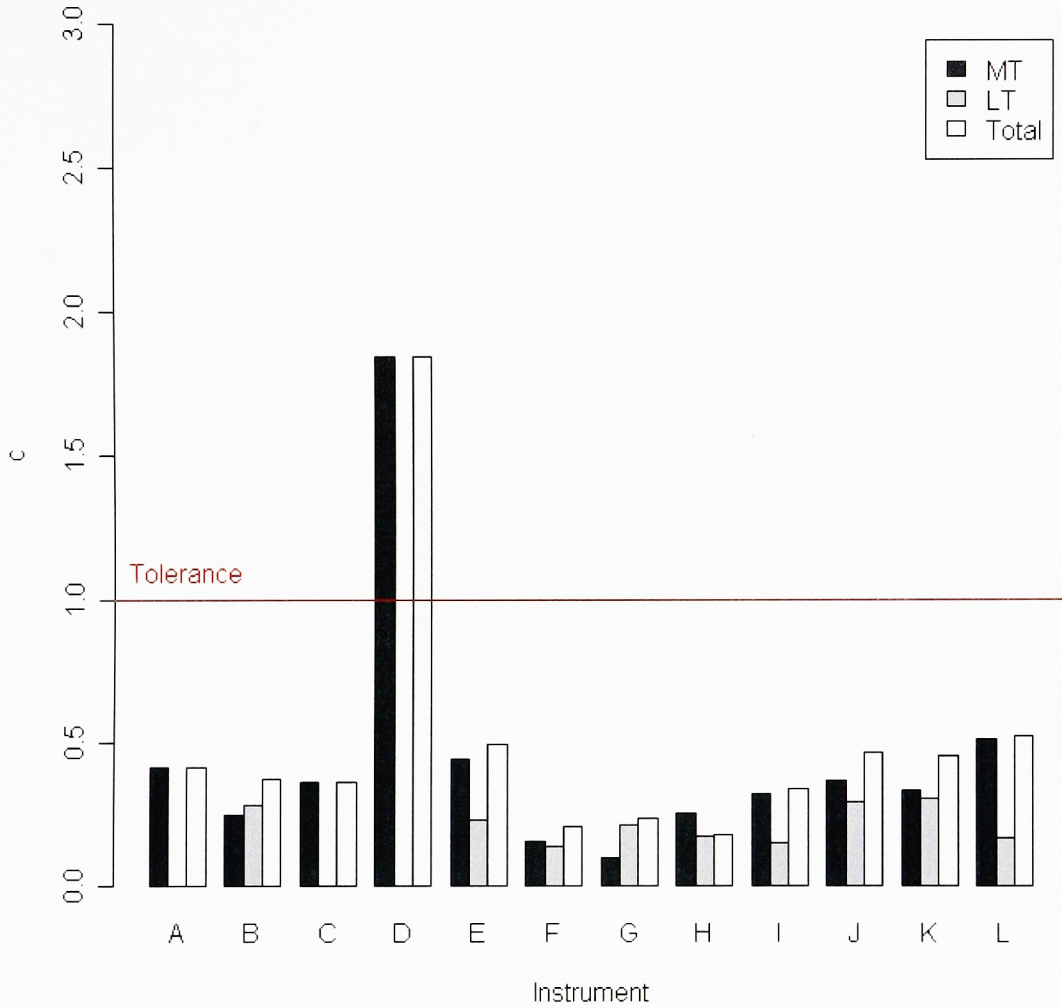


Figure 17 is a plot of the data and tolerance region. Figure 18 depicts the results obtained for instrument A. As the LT variance component resulted non significant, the ST variance component is equal to the total variance.

Figure 17. Data and tolerance region, instrument A, Example 3.

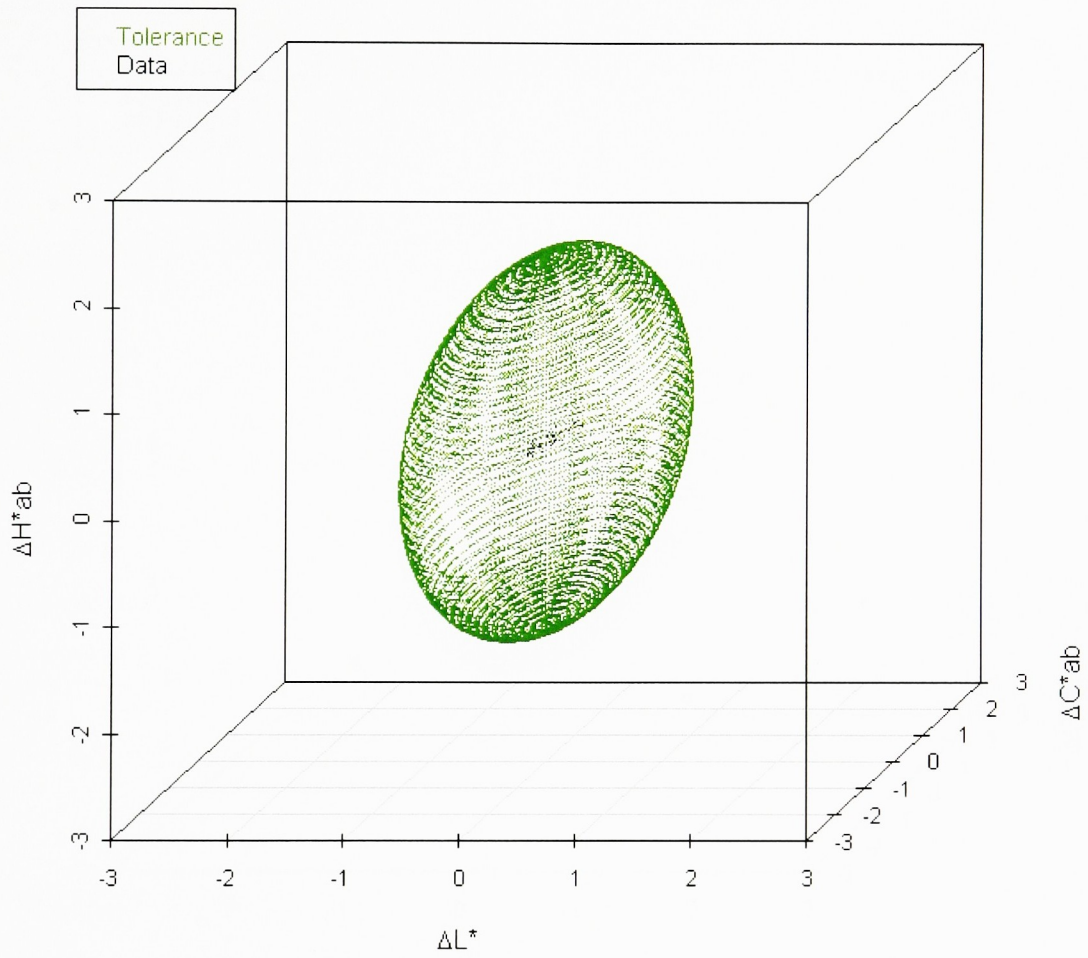
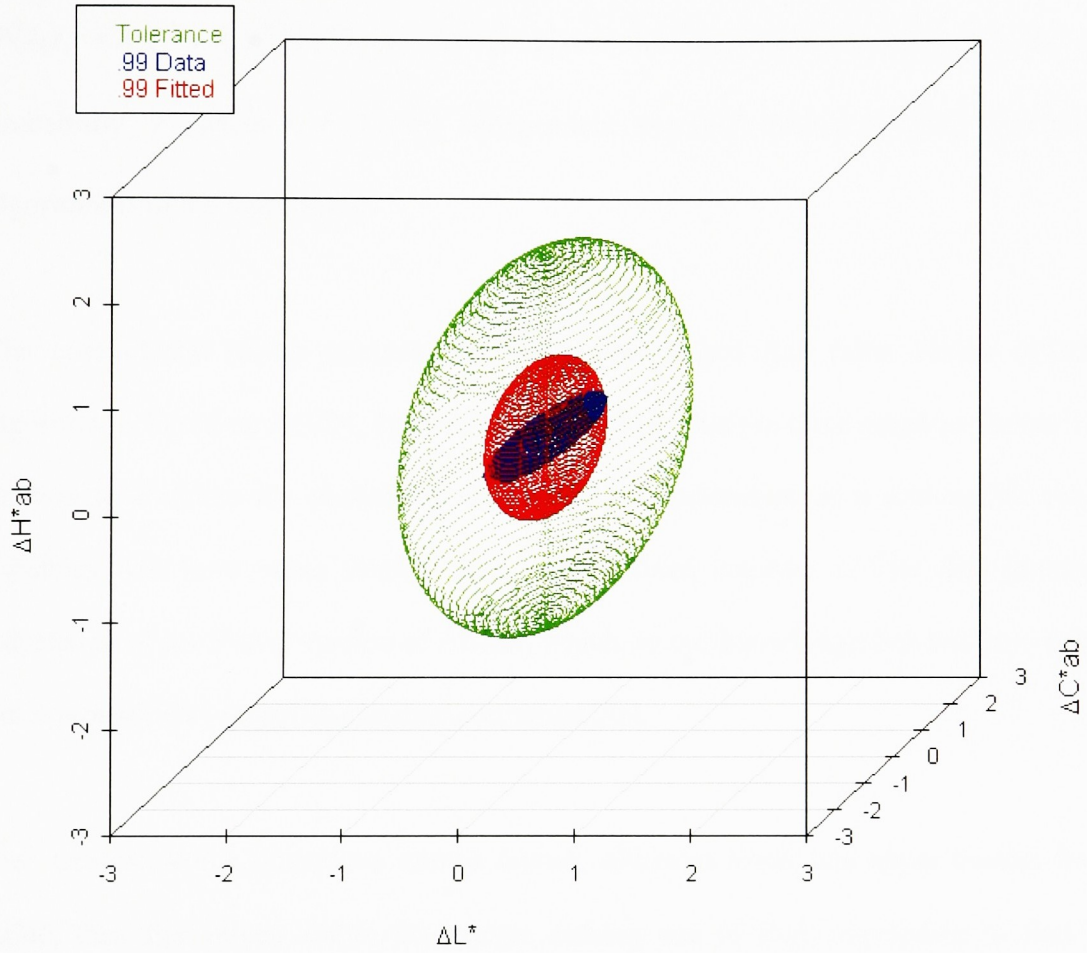


Figure 18. Tolerance, .99 natural capture ellipsoid and .99 capture fitted ellipsoid, instrument A, Example 3.



Appendix 1

The algorithm is an iterative search procedure, used in solving $P(\lambda_1 Y_1^2 + \lambda_2 Y_2^2 + \lambda_3 Y_3^2 \leq c^2) = \gamma$ for c , given the eigenvalues $\lambda_1, \lambda_2, \lambda_3$ and the desired probability γ , where Y_1, Y_2, Y_3 are independent standard normal random variables. The algorithm is in the language R.

The core of the search procedure is a function named *Rub* (after Ruben (1962)); the algorithm is based on AS204, by Farebrother (1984), which in turns employs Ruben's (1962) method to evaluate the probability that a linear combination of n non-central chi-square variables will have value smaller than a pre-defined constant c . The *Rub* function is a translation of the Pascal version of AS204, which, to our knowledge, has not been published, but is available at: <http://lib.stat.cmu.edu/apstat/204>.

The iterative search procedure, named *Invrub*, estimates lower and upper bounds for the c value, then fits values within that range, making use of *Rub*, attempting to find c for a given γ . Those upper and lower bounds are calculated observing that c^2 in $P(\lambda_1 y_1^2 + \lambda_2 y_2^2 + \lambda_3 y_3^2 \leq c^2) = \gamma$ has to be in the range (c_{\max}^2, c_{\min}^2) , where: $c_{\max}^2 = \chi_{3,(1-\gamma)}^2 \lambda_1$. Similarly, $c_{\min}^2 = \chi_{3,(1-\gamma)}^2 \lambda_3$.

For example, if we wished to calculate $P(.3y_1^2 + .2y_2^2 + .1y_3^2 \leq 1)$, we could employ the function *Rub* with the following call: `Rub(c(.3, .2, .1), 1)`.

The output obtained is γ and a fault code (please note, fault codes are those used by AS204 (Farebrother (1984))):

Any negative fault code indicates that one or more of the constraints $\lambda_i > 0, m_i > 0$ and $\delta_i^2 \geq 0$ is not satisfied;

1 = non-fatal underflow;

2 = one or more of the constraints $n > 0, c > 0, eps > 0$ and $maxit > 0$ is not satisfied;

3 = the current estimate of the probability is less than -1;

4 = the required level of precision could not be obtained in $maxit$ iterations;

5 = the value returned by the procedure is not between 0 and 1 (extremes included);

6 = the estimated γ is negative;

9 = faults 4 and 5;

10 = faults 4 and 6;

0 = otherwise;

Similarly, if we wanted to find the c for which $P(0.3y_1^2 + 0.2y_2^2 + 0.1y_3^2 \leq c^2) = .99$, we could employ the function *Invrub* with the following call: `Invrub(c(.3, .2, .1), .99)`.

The *Invrub* function offers, as output, c^2 , γ (the exact capture rate), the fault code obtained with the last iteration of *Rub* and a binary indicator variable. The latter is set to 0 if the required level of precision is attained, or 1 if the required level of precision was not attained (in which case, the code can be easily modified for allowing a higher number of iterations, as indicated in the program comments).

The function Rub

```
Rub<-function(lambda, cc)

# Farebrother, R.W. (1984), [AS 204] The Distribution of a Positive Linear
# Combination of Chi-Square Random Variables, Royal Statistical Society
# (Series C), Vol. 33, No. 3 1984, pp. 332-339. #

{degcount=0
for (i in 1:3)
  {if (lambda[i]==0) {templ=degcount; degcount=templ+1};}
n = 3-degcount
maxit = 2000
eps = .001
mode = 0.90625
exit2=0
delta <- array(dim=c(n))
for (i in 1:n) {delta[i] = 0}
mult <- array(dim=c(n))
gamma <- array(dim=c(n))
theta <- array(dim=c(n))
a <- array(dim=c(maxit))
b <- array(dim=c(maxit))
for (i in 1:n) mult[i] = 1
exit = 0
L = 0
if (n==0) {RUBEN=0; ifault=0; exit=1} else
{if (n < 1 | cc<=0 | maxit<1 | eps <=0)
  {RUBEN=-2; ifault =2}
  {tol=-200;
  beta =lambda[1];
  sum=lambda[1];
  for(i in 1:n)
    {hold=lambda[i];
    if (hold <=0 | mult[i]<1 | delta[i]<0)
      {RUBEN = -7;
      ifault = -i;
      exit = 1;
      i = n;};}
    if (beta>hold) beta=hold;
    if (sum<hold) sum=hold;};}
if (exit == 0)
  {if(mode>0)
    {temp=mode*beta;beta=temp} else
    {temp=2/(1/beta+1/sum);beta=temp};
  k=0;sum=1;suml=0;
  for(i in 1:n)
    {hold=beta/lambda[i]; gamma[i]=1-hold;temp=1;
    for (j in 1:mult[i]) {temp=temp*hold};
    sum=sum*temp; suml=suml+delta[i];k=k+mult[i];theta[i]=1};
  ao=exp(.5*(log(sum)-suml));
  if (ao<=0)
    {reuben=0;dnsty=0;ifault=1} else
    {z=cc/beta; itemp=(k%/%2)*2;
```

```

if (k==itemp)
    {i=2;lans=-.5*z;dans=exp(lans);pans=1-dans} else
    {i=1;
    lans=-.5*(z+log(z))-0.22579135264473;dans=exp(lans);
    rz=sqrt(z);pans=( pnorm (rz,0,1,TRUE,FALSE)- pnorm (-
rz,0,1,TRUE,FALSE));
    k= k - 2;
    while (i <= k)
        {if (lans < tol)
            {lans = lans + log(z/i);dans = exp(lans)} else
            {temp = dans; dans = temp * z/i};
            temp=pans;pans=temp-dans;i=i+2};
    prbty=pans;dnsty=dans;eps2=eps/ao;aoinv=1/ao;sum=aoinv-1;
    for (m in 1:maxit)
        {if(exit2==0)
            {sum1 = 0.0;
            for (i in 1:n)
                {hold = theta[i];
                theta[i] = hold * gamma[i];
                hold2 = theta[i];
                temp = hold2 * mult[i] + m * delta[i] *
(hold - hold2);
                sum1 = sum1 + temp};
            b[m] = 0.5 * sum1;
            sum1 = b[m];
            itemp = m - 1;
            if (itemp > 0)
                {for (i in itemp:1)
                    {sum1 = sum1 + b[i] * a[m-i]}};
            a[m] = sum1/m;
            sum1 = a[m];
            k = k + 2;
            if (lans < tol)
                {lans = lans + log(z/k);
                dans = exp(lans)} else
                {temp = dans;
                dans = temp * z/k;}
            pans = pans - dans;
            sum = sum - sum1;
            temp = dnsty;
            dnsty = temp + dans * sum1;
            temp = sum1;
            sum1 = pans * temp;
            temp = prbty;
            prbty = temp + sum1;
            if (prbty < -aoinv)
                {RUBEN = -3.0;
                ifault = 3;
                exit = 1;
                m = maxit;}
            if (exit == 0)
                {temp = abs(pans* sum);
                if (temp < eps2)
                    {temp = abs(sum1);
                    if (temp < eps2)
                        {ifault = 0;

```

```

                                L = 1;
                                m = maxit;exit2=1}}};};
                                };
                                };
};
if (L == 0) {ifault = 4};
if (exit == 0)
    {temp = dnsty;
    dnsty = ao * temp/(beta + beta);
    temp = prbty;
    prbty = ao * temp;
    if (prbty < 0.0 | prbty > 1.0)
        ifault = ifault + 5} else
        {if (dnsty < 0.0) {ifault = ifault + 6}}};};
    RUBEN = prbty;}

RUBEN
test=c(RUBEN, ifault)
test}

```

The function Invrub

```

Invrub<-function(lambdal,crate)
{minlambda=min(lambdal[1],lambdal[2],lambdal[3])
maxlambda=max(lambdal[1],lambdal[2],lambdal[3])
cmin=qchisq(1-crate,3,FALSE,FALSE)*minlambda
cmax=qchisq(1-crate,3,FALSE,FALSE)*maxlambda
cfirst=(cmax+cmin)/2
exitl=1
precision = .00001           #sets the level of precision#
maxnit=100                   #sets the maximum number of iterations#
for (counter in 1:maxnit)
    {if (exitl==1)
        {a=Rub(lambdal,cfirst)
        prec=(cmax-cmin)/2
        deviation = crate-a[1]
        if (prec > precision)
            {if (deviation > 0)
                {cmin=cfirst; cfirst=(cfirst+cmax)/2} else
                {cmax=cfirst; cfirst=(cfirst+cmin)/2}}
            else {exitl=0}}};}
b=Rub(lambdal,cfirst)
d=exitl
e=c(cfirst,b[1],d,b[2])
e}

```

Appendix 2

The algorithm presented here is meant to automate the computation of the proposed process capability index in the field of color metrics. It attempts to estimate the process capability index by making use of the CIE_{94} equations presented in the *Application: analysis of color metrics* section.

The following algorithm has been developed as well for the statistical package R. It makes use of the two algorithm presented in *Appendix 1*, *Rub* and *Invrub*. In addition, it requires the package `scatterplot3d`¹ to be installed and loaded. The function requires the following input parameters:

VarCovar the variance-covariance matrix for the variance component of interest

Amean the mean observed value for a^*

Bmean the mean observed value for b^*

Gamma the desired capture rate

The algorithm output will include: c (the process capability index), c^2 , the exact capture rate associated with that c and two fault codes, associated, respectively, with the algorithms *Rub* and *Invrub* (if fault codes are different from zero, we recommend increasing the number of maximum allowed iterations in the respective algorithms). Finally, the algorithm offers a three-dimensional plot presenting the γ capture region associated with the variance-

¹ Available at <http://www.r-project.org/>

covariance matrix, the tolerance region and the γ capture region with the same shape and orientation of the tolerance region.

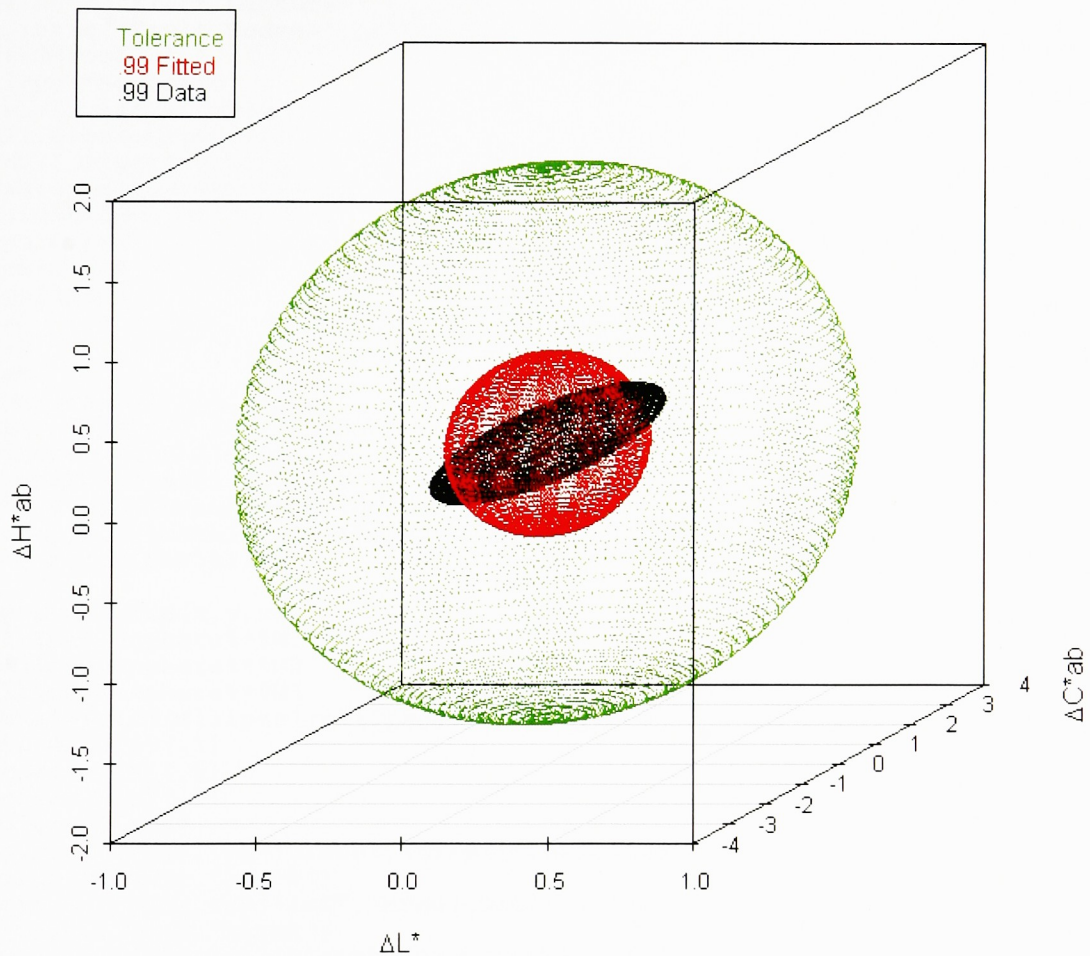
For example, the following call, using the parameters for *Example 3*, Instrument A:

```
pci(matrix(c(0.013248, .0043168, .0093528, .0043168, .007848, .0017508, .0093528, .0017508, .0124696), 3, 3), -28.360494, -38.42449, .99)
```

will produce the plot presented in Figure 19 and the following output:

```
[1] "c=" "0.329637830095298"  
[1] "c^2=" "0.108661099029937"  
[1] "Exact Capture=" "0.99000098123337"  
[1] "Fault Codes=" "0" "0"
```

Figure 19. Output of the *Pci* algorithm.



The function Pci

```

pci<-function(VarCovar, Amean, Bmean, Gamma)
{Cabmean=((Amean^2)+(Bmean^2))^(.5)
Sl=1
Sc=1+0.045*Cabmean
Sh=1+0.015*Cabmean
MaxDim=max(Sl, Sh, Sc)
SqrtTol=matrix(c(Sl, 0, 0, 0, Sc, 0, 0, 0, Sh), 3, 3)
InvSqrtTol=chol2inv(chol(SqrtTol))
U1=InvSqrtTol%*%VarCovar
U=U1%*%InvSqrtTol
values1=eigen(U)$values
values2=sort(values1)
}

```

```

values=c(values2[3],values2[2],values2[1])
pcisq=Invrub(values,Gamma)
pci=sqrt(pcisq[1])
print(c("c=",pci))
print(c("c^2=",pcisq[1]))
print(c("Exact Capture=",pcisq[2]))
print(c("Fault Codes=",pcisq[3],pcisq[4]))
M1=SqrootTol
M2=pci*SqrootTol
m31=11.34*VarCovar
m31.eigen=eigen(m31)
C=m31.eigen$vectors
D=diag(m31.eigen$values)
M3=C%*%sqrt(D)%*%t(C)
xpoints=0
ypoints=0
zpoints=0
x=0
y=0
z=0
for (thetali in 0:100)
{for (theta2i in -75:75)
{thetal=(thetali+0)*3.6
theta2=(theta2i+75)*1.8
x=c(x,sin(thetal)*cos(theta2))
y=c(y,sin(thetal)*sin(theta2))
z=c(z,cos(thetal))}
}
sphere=cbind(x,y,z)
ellipse1=sphere%*%M1
ellipse2=sphere%*%M2
ellipse3=sphere%*%M3
total=rbind(ellipse1,ellipse2,ellipse3)
xcord=total[,1]
ycord=total[,2]
zcord=total[,3]
color="black"
color=c(color,rep("green",(nrow(total)-3)/3))
color=c(color,"black")
color=c(color,rep("red",(nrow(total)-3)/3))
color=c(color,"black")
color=c(color,rep("black",(nrow(total)-3)/3))
color=c(color,rep("black",0))
scatterplot3d(xcord,ycord,zcord,color, pch='.',
xlab=expression(paste(Delta,'L*')),ylab=expression(paste(Delta,'C*ab')),zla
b=expression(paste(Delta,'H*ab')), scale.y=.5,angle=45)
legend("topleft",c("Tolerance","Fitted",
"Natural"),text.col=c("green","red","black"),cex=.90)}

```

Appendix 3. Data assumption checking, instrument I, long-term data, cyan.

To illustrate the procedure applied when exploring the datasets used in the example, we report the process applied to the long term dataset, cyan tile, for the first handheld bidirectional instrument (instrument I).

Univariate plots of the data versus order of observations are presented in Figure 20, Figure 21 and Figure 22. The results of formal univariate normality tests are presented in Table 11, Table 12 and Table 13.

Figure 20. Lightness versus time, long-term, cyan, instrument I.

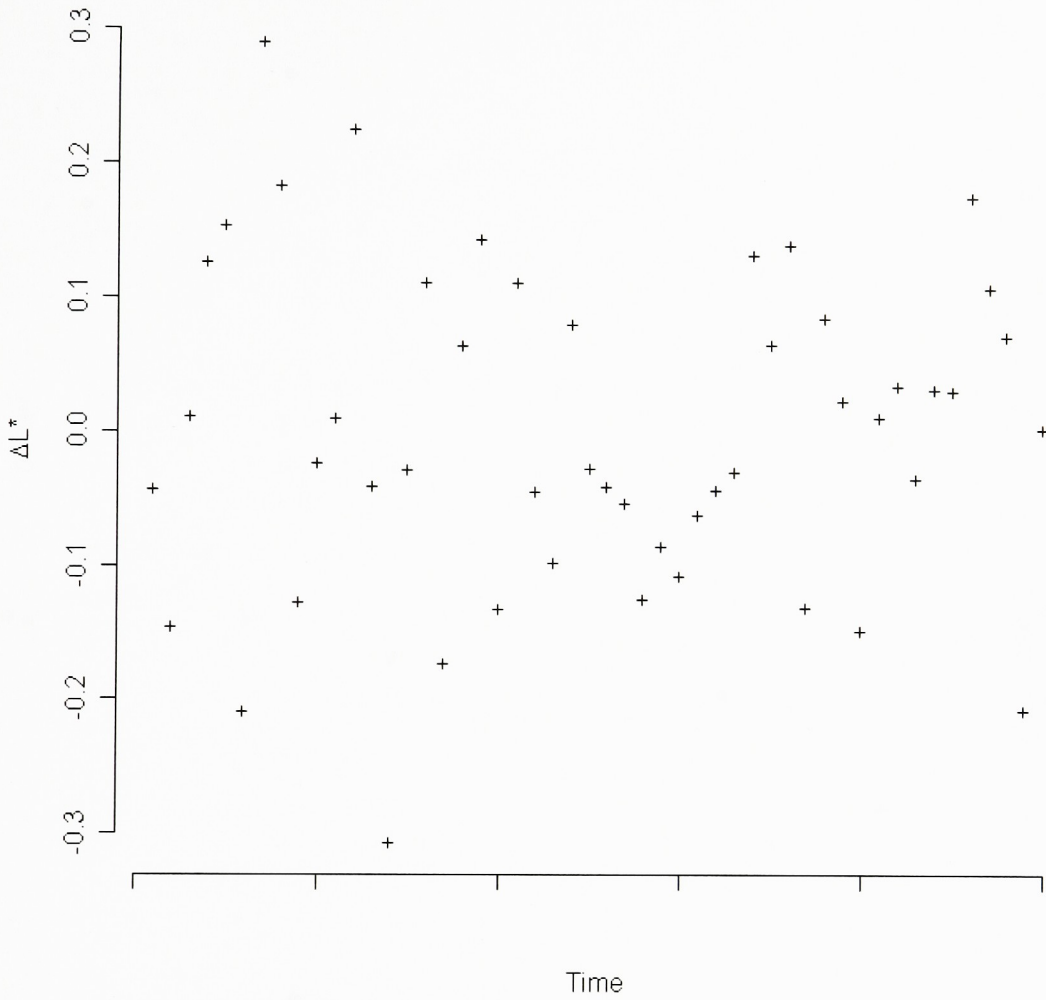


Figure 21. Chroma versus time, long-term, cyan, instrument I.

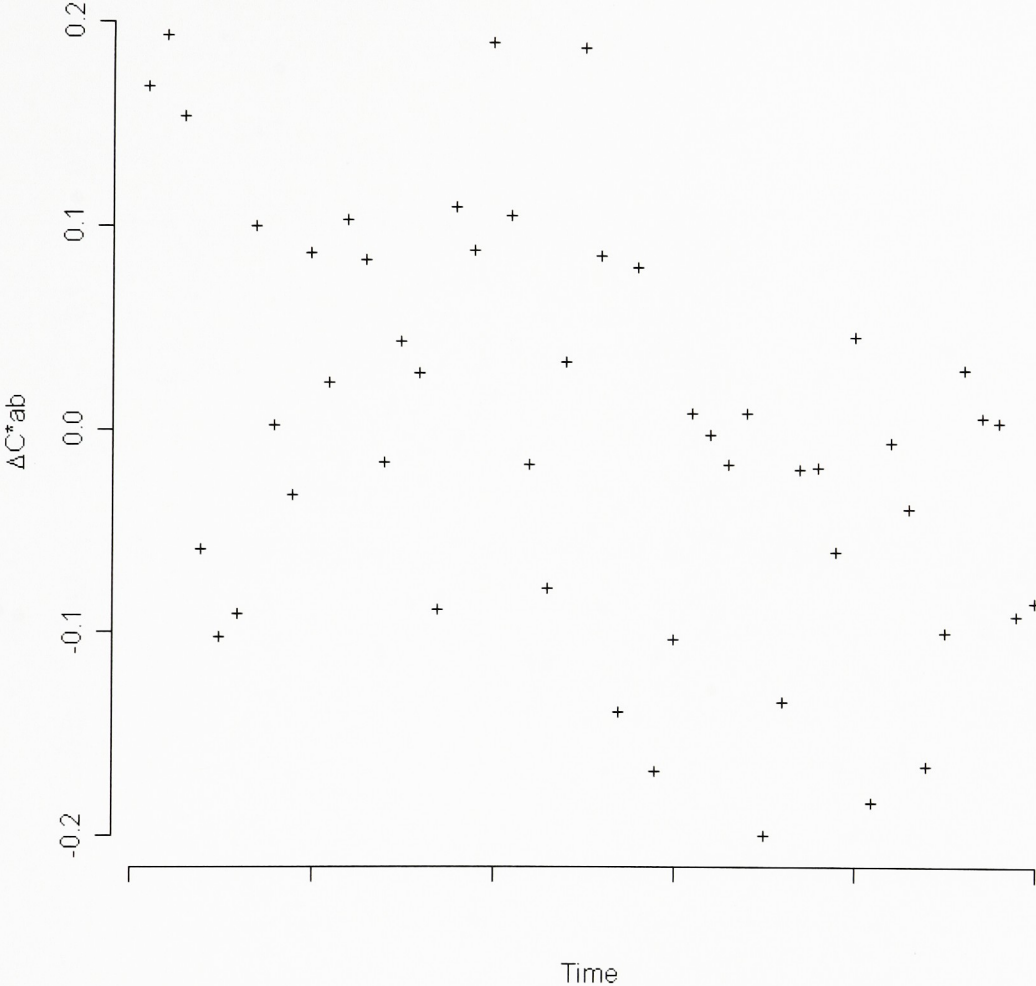


Figure 22. Hue versus time, long-term, cyan, instrument I.

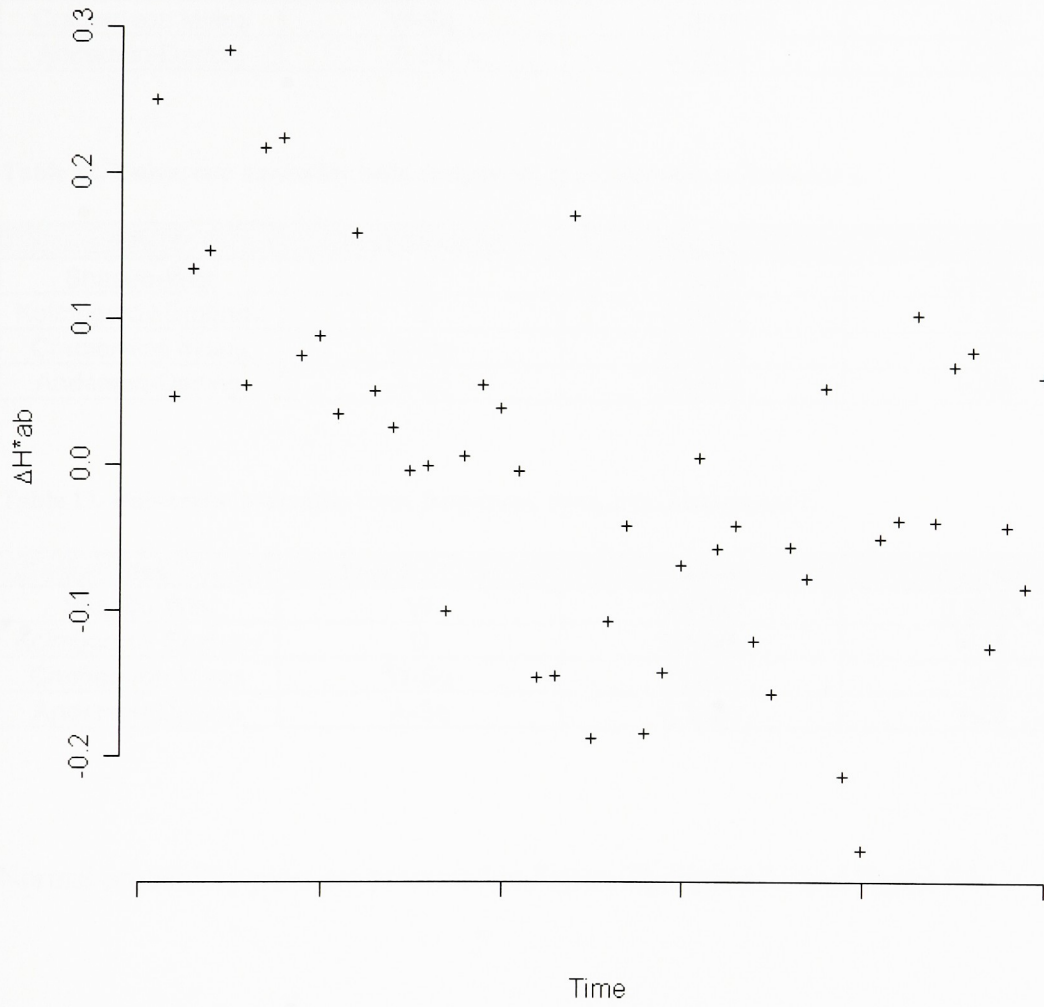


Table 11. Univariate normality tests, long-term, cyan, lightness, instrument I.

Test	Test Statistic	Value	P-value
Shapiro-Wilk	W	0.9900	0.9921
Kolmogorov-Smirnov	D	0.0742	>.15
Cramer-von Mises	W-Sq	0.0316	>.25
Anderson-Darling	A-Sq	0.1815	>.25

Table 12. Univariate normality tests, long-term, cyan, chroma, instrument I.

Test	Test Statistic	Value	P-value
Shapiro-Wilk	W	0.9700	0.3475
Kolmogorov-Smirnov	D	0.0453	>.15
Cramer-von Mises	W-Sq	0.0375	>.25
Anderson-Darling	A-Sq	0.2600	>.25

Table 13. Univariate normality tests, long-term, cyan, hue, instrument I.

Test	Test Statistic	Value	P-value
Shapiro-Wilk	W	0.9800	0.8233
Kolmogorov-Smirnov	D	0.0746	>.15
Cramer-von Mises	W-Sq	0.0287	>.25
Anderson-Darling	A-Sq	0.1938	>.25

Normal probability plots are presented in Figure 23, Figure 24 and Figure 25.

Figure 23. Normal probability plot, long-term, cyan, instrument I, lightness.

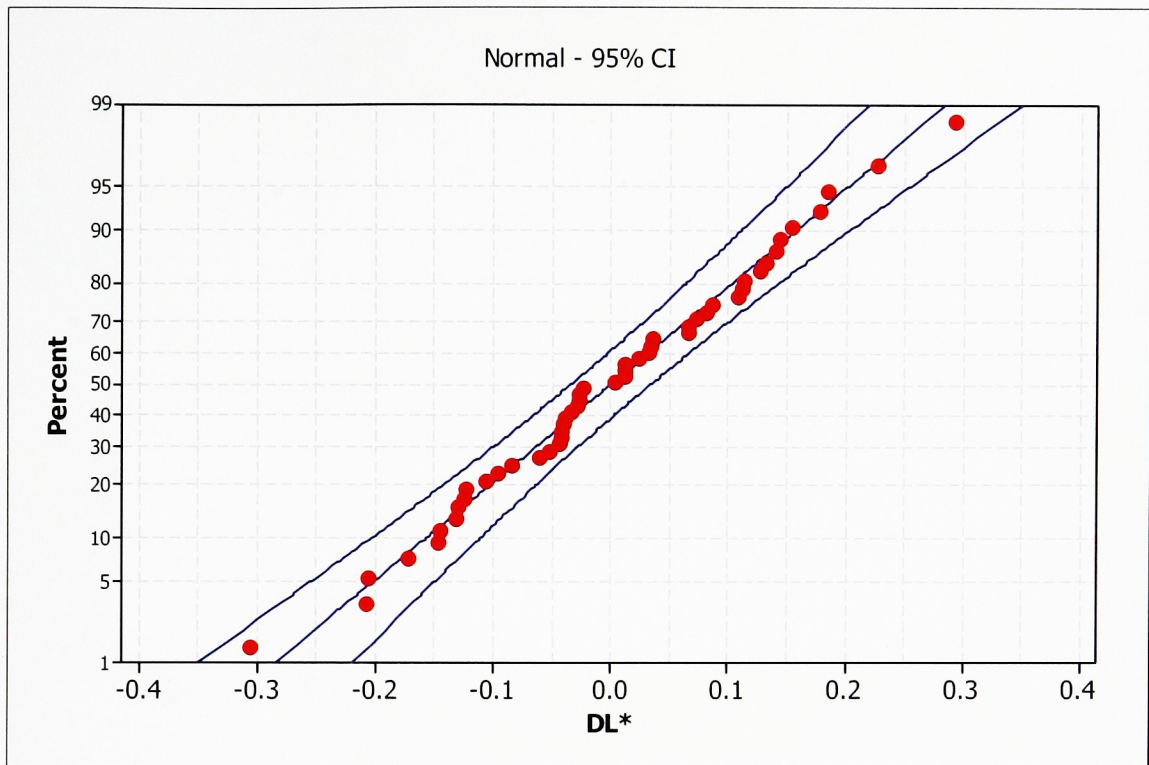


Figure 24. Normal probability plot, long-term, cyan, instrument I, chroma.

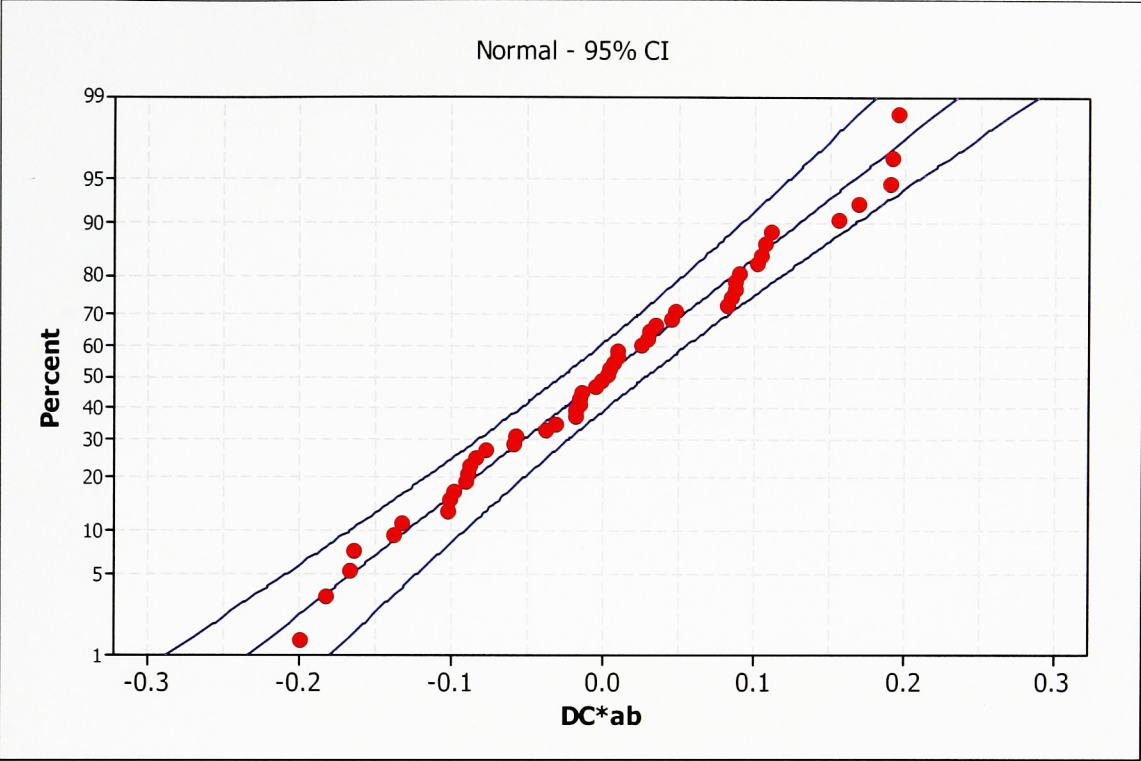
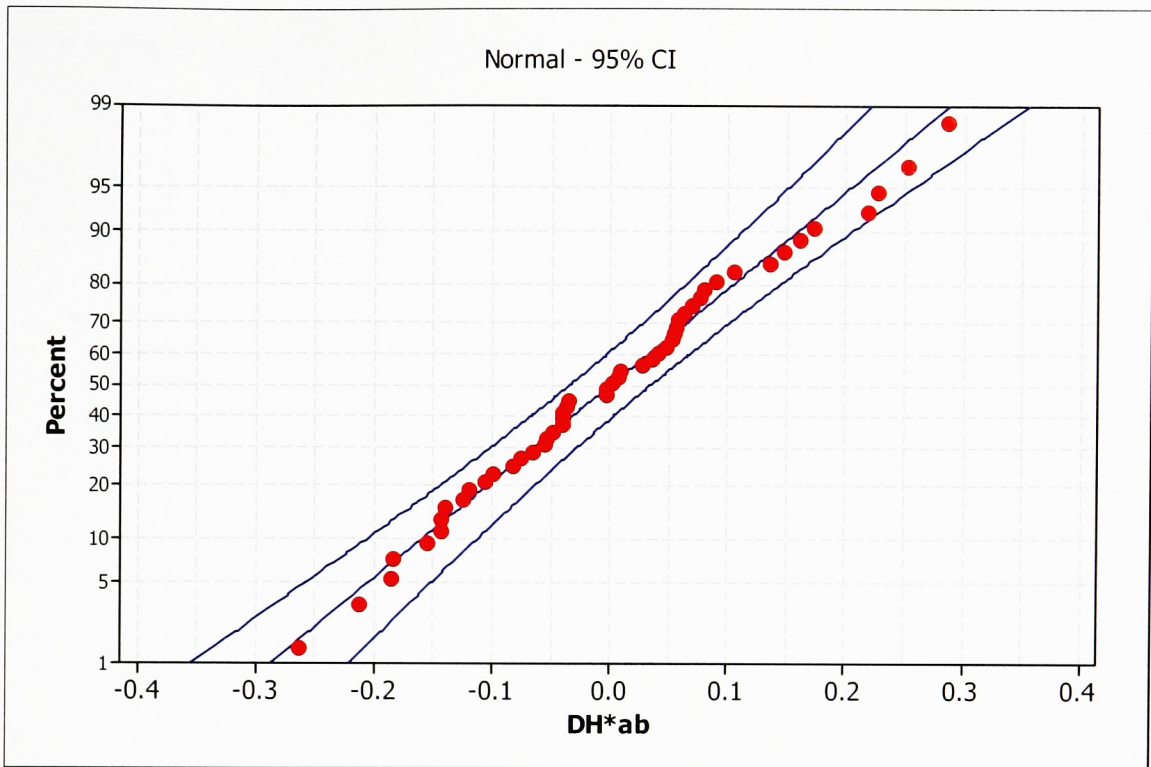


Figure 25. Normal probability plot, long-term, cyan, instrument I, hue



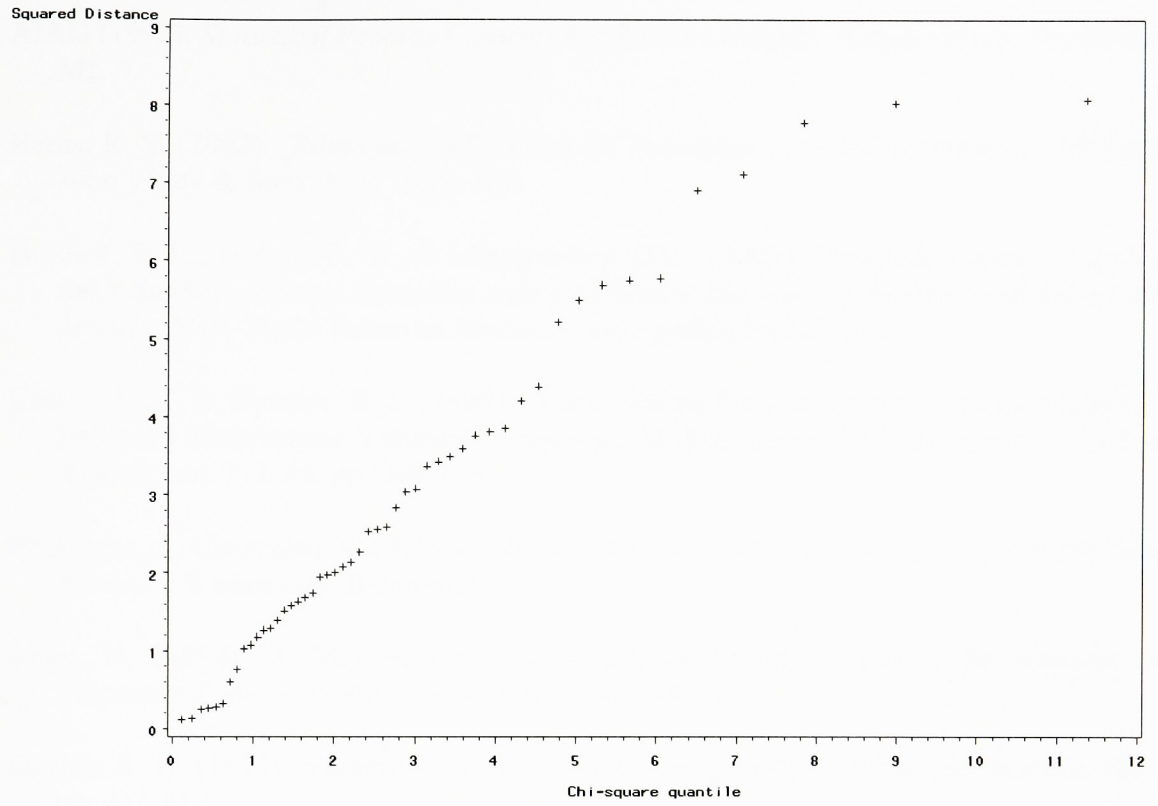
Formal tests for normality for the multivariate set presented in Table 14 detected no significant skewness or kurtosis at a level of confidence of .05. Finally, the Henze-Zirkler T-test did not detect any significant departure from normality at a level of confidence of .05.

A chi-square Q-Q plot presented in Figure 26 confirms the findings.

Table 14. Multivariate tests.

Test	Value	P-value
Mardia Skewness	5.24	0.8748
Mardia Kurtosis	-0.67	0.5022
Henze-Zirkler T	-1.39	0.1658

Figure 26. Chi-square Q-Q plot, long term, cyan, instrument I.



References

- AIAG (1992). *Statistical Process Control*, Automotive Industry Action Group, Southfield, MI.
- Berns, R. S. (2002). *Billmeyer and Saltzman's Principles of Color Technology*, 3rd Edition, John Wiley & Sons, New York, NY.
- Burdick, R. K., Borror, C. M., & Montgomery, D.C., (2005). *Design and Analysis of Gauge R&R Studies: Making Decisions with Confidence Intervals in Random and Mixed Anova Models*, ASA-SIAM Series on Statistics and Applied Probability.
- Calvin, J. A., & Dykstra, R. L., (1991). Least Square Estimation of Covariance Matrices in Balanced Multivariate Variance Component Models, *Journal of the American Statistical Association*, Vol. 86, pp. 388-395.
- Chambers, J., Cleveland, W., Kleiner, B., & Tukey, P. (1983), *Graphical Methods for Data Analysis*, Wadsworth, Belmont, CA.
- Chen, H. (1994). A Multivariate Process Capability Index Over a Rectangular Solid Tolerance Zone, *Statistica Sinica*, Vol. 4, pp. 749-758.
- Davies, R. B. (1973). Numerical inversion of a characteristic function, *Biometrika*, Vol. 60, pp. 415-417.
- Davies, R. B. (1980). [AS 155] The Distribution Function of a Linear Combination of χ^2 Random Variables, *Applied Statistics*, Vol. 29, pp. 323-333.
- Demeter, L. (1989). *Improvements Needed to Elevate the State of the Art to Meet Evolving Industry Quality Standards*, Technical Paper 898772, Society of Automotive Engineers, Warrendale, Pennsylvania.
- Farebrother, R.W. (1984). [AS 204] The Distribution of a Positive Linear Combination of χ^2 Random Variables, *Journal of the Royal Statistical Society (Series C)*, Vol. 33, No. 3, pp. 332-339.
- Grad, A., & Solomon, H., (1955), Distribution of Quadratic Forms and Some Applications, *Annals of Mathematical Statistics*, Vol. 26, pp. 464-477.
- Guenther, W. C., & Terragno, P.J., (1964). A Review on the Literature on a Class of Coverage Problems, *Annals of Mathematical Statistics*, Vol. 35, pp. 232-242.
- Henze, N. and Zirkler, B. (1990). A Class of Invariant Consistent tests for Multivariate Normality, *Communication in Statistics – Theory and Methods*, Vol. 19, pp. 3595-3617.

- Hulting, F.L. (1992). Methods for the Analysis of Coordinate Measurement Data, *Computing Science and Statistics, Vol. 24*, pp. 160-169.
- Mardia (1980). Measures of Multivariate Skewness and Kurtosis with Applications, *Biometrika Vol. 57*.
- Marsiglia, G. (1960). *Tables of the Distribution of Quadratic Forms of Ranks Two and Three*, Boeing Scientific Research Laboratories, Report No. D1-82-0015-1, Seattle, WA.
- Montgomery, D. C. (2005). *Design and Analysis of Experiments*, Fifth Edition, Wiley, New York, NY.
- Jobson, J.D., (1999). *Applied Multivariate Data Analysis, Volume 1: Regression and Experimental Design*, Springer Texts in Statistics, New York, NY.
- Johnson, R. A., & Wichern, D. W. (2002), *Applied Multivariate Statistical Analysis*, Fifth Edition, Prentice Hall.
- Johnson, N. L., & Kotz, S (1968). Tables for the distributions of positive definite quadratic forms in central normal variables, *Shankya, Series B, Vol. 30*, pp. 303-314.
- Johnson, N. L., Kotz, S. & Balakrishnan, N. (1994). *Continuous Univariate Distributions*, Vol 2, Second Edition, pp. 444-450, Wiley, New York, NY.
- Kotz, S., & Johnson, N.L. (2002). Process capability indices – a review, 1992-2000, *Journal of Quality Technology, Vol. 34*, No.1, (January 2002), pp. 2-53.
- Ryan, T.A., & Joiner, B.A. (1976). *Normal Probability Plots and Tests for Normality*, Technical Report, Statistics Department, The Pennsylvania State University.
- Rencher, A.C., (2002). *Methods of Multivariate Analysis*, 2nd Edition, Wiley, New York, NY.
- Ruben, H. (1962). Probability content of regions under spherical normal distributions. IV The distribution of homogeneous and non-homogeneous quadratic functions of normal variables, *Annals of Mathematical Statistics, Vol. 33*, pp. 542-570.
- Seves, R. (1996). Practical Formula for the Computation of CIE 1976 Hue Differences, *Color Res. Applied, Vol. 21*, page 314.
- Shahriari, H., Hubele, N.F. and Lawrence, F.P. (1995), *A Multivariate Process Capability Vector*, Proceedings of the 4th Industrial Engineering Research Conference, Institute of Industrial Engineers, pp. 304-309.
- Shapiro, S.S., & Wilk, M.B. (1965). An Analysis of Variance Test for Normality (complete samples), *Biometrika, 52*.

- Sheil, J., & O'Muircheartaigh, I. (1977), The Distribution of Non-Negative Quadratic Forms in Normal Variables, *Applied Statistics*, Vol. 26, Number 1.
- Solomon, H. (1960). *Distribution of Quadratic Forms, Tables and Applications*, Applied Mathematics and Statistics Laboratories, Stanford University, Technical Report No. 45, Stanford, CA.
- Solomon, H. & Stephens, M.A. (1977). Distribution of a sum of weighted chi-square variables, *Journal of the American Statistical Association*, Vol. 72, pp. 881-885.
- Stokes, M., Fairchild, D., & Berns, R.S. (1992). Colorimetric Quantified Tolerances for Pictorial Images, *Proc. Tech. Assoc. Graphic, Arts Vol. 2*, pp. 757-778.
- Voelkel, J.G. (2003). Gauge R&R Analysis for Two-Dimensional Data with Circular Tolerances, *Journal of Quality Technology*, Vol. 35, No. 2, pp. 153-167.
- Völz, H.G., (1995). *Industrial Color Testing – Fundamentals and Techniques*, Second Edition, Wiley New York, NY.
- Wang, F. K, Hubele, N. F., Lawrence, F. P., Miskluin, J. D., & Shahriari, H. (2000), Comparison of Three Multivariate Process Capability Indices, *Journal of Quality Technology*, Vol. 32, pp. 263-275.
- Wheeler, D. J., & Lyday, W., (1989). *Evaluating the Measurement Process*, 2nd Edition, SPC Press, Knoxville, TN.

Filename: Draft V5.doc
Directory: F:\Thesis
Template: C:\Documents and
Settings\FASTKiosk_XRDS\Application
Data\Microsoft\Templates\Normal.dot
Title: We consider gauge repeatability and reproducibility (R&R)
analysis for three-dimensional data
Subject:
Author: vxf6971
Keywords:
Comments:
Creation Date: 12/7/2005 8:04:00 PM
Change Number: 7
Last Saved On: 12/8/2005 12:40:00 PM
Last Saved By: ogb
Total Editing Time: 49 Minutes
Last Printed On: 12/8/2005 1:03:00 PM
As of Last Complete Printing
Number of Pages: 84
Number of Words: 12,059 (approx.)
Number of Characters: 68,742 (approx.)